19 PRESTRESSED CONCRETE

19.1 INTRODUCTION

Modern structural engineering tends to progress toward more economical structures through gradually improved methods of design and the use of higher-strength materials. This results in a reduction of cross-sectional dimensions and consequent weight savings. Such developments are particularly important in the field of reinforced concrete, where the dead load represents a substantial part of the total load. Also, in multistory buildings, any saving in depth of members, multiplied by the number of stories, can represent a substantial saving in total height, load on foundations, length of heating and electrical ducts, plumbing risers, and wall and partition surfaces.

Significant savings can be achieved by using high-strength concrete and steel in conjunction with present-day design methods, which permit an accurate appraisal of member strength. However, there are limitations to this development, due mainly to the interrelated problems of cracking and deflection at service loads. The efficient use of high-strength steel is limited by the fact that the amount of cracking (width and number of cracks) is proportional to the strain, and therefore the stress, in the steel. Although a moderate amount of cracking is normally not objectionable in structural concrete, excessive cracking is undesirable in that it exposes the reinforcement to corrosion, it may be visually offensive, and it may trigger a premature failure by diagonal tension. The use of high-strength materials is further limited by deflection considerations, particularly when refined analysis is used. The slender members that result may permit deflections that are functionally or visually unacceptable. This is further aggravated by cracking, which reduces the flexural stiffness of members.

These limiting features of ordinary reinforced concrete have been largely overcome by the development of prestressed concrete. A prestressed concrete member can be defined as one in which there have been introduced internal stresses of such magnitude and distribution that the stresses resulting from the given external loading are counteracted to a desired degree. Concrete is basically a compressive material, with its strength in tension being relatively low. Prestressing applies a precompression to the member that reduces or eliminates undesirable tensile stresses that would otherwise be present. Cracking under service loads can be minimized or even avoided entirely. Deflections may be limited to an acceptable value; in fact, members can be designed to have zero deflection under the combined effects of service load and prestress force. Deflection and crack control, achieved through prestressing, permit the engineer to make use of efficient and economical high-strength steels in the form of strands, wires, or bars, in conjunction with concretes of much higher strength than normal. Thus, prestressing results in the overall improvement in performance of structural concrete used

for ordinary loads and spans and extends the range of application far beyond the limits for ordinary reinforced concrete, leading not only to much longer spans than previously thought possible, but permitting innovative new structural forms to be employed.

19.2 Effects of Prestressing

There are at least three ways to look at the prestressing of concrete: (a) as a method of achieving *concrete stress control*, by which the concrete is precompressed so that tension normally resulting from the applied loads is reduced or eliminated, (b) as a means for introducing *equivalent loads* on the concrete member so that the effects of the applied loads are counteracted to the desired degree, and (c) as a *special variation of reinforced concrete* in which prestrained high-strength steel is used, usually in conjunction with high-strength concrete. Each of these viewpoints is useful in the analysis and design of prestressed concrete structures, and they will be illustrated in the following paragraphs.

a. Concrete Stress Control by Prestressing

Many important features of prestressed concrete can be demonstrated by simple examples. Consider first the plain, unreinforced concrete beam with a rectangular cross section shown in Fig. 19.1*a*. It carries a single concentrated load at the center of its span. (The self-weight of the member will be neglected here.) As the load W is gradually applied, longitudinal flexural stresses are induced. If the concrete is stressed only within its elastic range, the flexural stress distribution at midspan will be linear, as shown.

At a relatively low load, the tensile stress in the concrete at the bottom of the beam will reach the tensile strength of the concrete f_r, and a crack will form. Because no restraint is provided against upward extension of the crack, the beam will collapse without further increase of load.

Now consider an otherwise identical beam, shown in Fig. 19.1*b*, in which a longitudinal axial force P is introduced prior to the vertical loading. The longitudinal prestressing force will produce a uniform axial compression $f_c = P/A_c$, where A_c is the cross-sectional area of the concrete. The force can be adjusted in magnitude so that, when the transverse load Q is applied, the superposition of stresses due to P and Q will result in zero tensile stress at the bottom of the beam as shown. Tensile stress in the concrete may be eliminated in this way or reduced to a specified amount.

It would be more logical to apply the prestressing force near the bottom of the beam, to compensate more effectively for the load-induced tension. A possible design specification, for example, might be to introduce the maximum compression at the bottom of the beam without causing tension at the top, when only the prestressing force acts. It is easily shown that, for a beam with a rectangular cross section, the point of application of the prestressing force should be at the lower third point of the section depth to achieve this. The force P, with the same value as before, but applied with eccentricity $e = h/6$ relative to the concrete centroid, will produce a longitudinal compressive stress distribution varying linearly from zero at the top surface to a maximum of $2f_c = P/A_c + Pec_2/I_c$ at the bottom, where f_c is the concrete stress at the concrete centroid, c_2 is the distance from the concrete centroid to the bottom of the

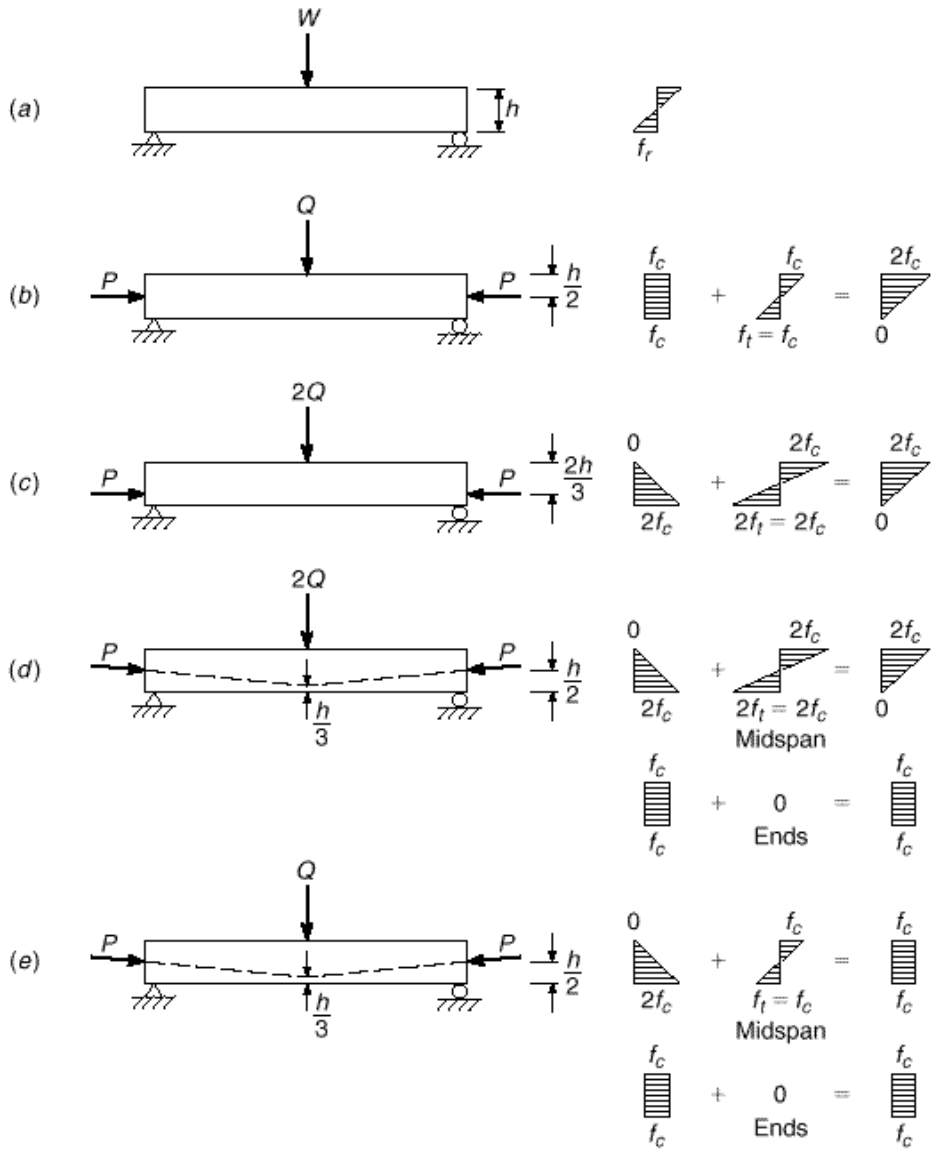

FIGURE 19.1
Alternative schemes for prestressing a rectangular concrete beam: (*a*) plain concrete beam; (*b*) axially prestressed beam; (*c*) eccentrically prestressed beam; (*d*) beam with variable eccentricity; (*e*) balanced load stage for beam with variable eccentricity.

beam, and I_c is the moment of inertia of the cross section. This is shown in Fig. 19.1*c*. The stress at the bottom will be exactly twice the value produced before by axial prestressing.

Consequently, the transverse load can now be twice as great as before, or $2Q$, and still cause no tensile stress. In fact, the final stress distribution resulting from the superposition of load and prestressing force in Fig. 19.1*c* is identical to that of Fig. 19.1*b*, with the same prestressing force, although the load is twice as great. The advantage of eccentric prestressing is obvious.

The methods by which concrete members are prestressed will be discussed in Section 19.3. For present purposes, it is sufficient to know that one practical method of prestressing uses high-strength steel tendons passing through a conduit embedded in the concrete beam. The tendon is anchored, under high tension, at both ends of the

beam, thereby causing a longitudinal compressive stress in the concrete. The prestress force of Fig. 19.1*b* and *c* could easily have been applied in this way.

A significant improvement can be made, however, by using a prestressing tendon with variable eccentricity with respect to the concrete centroid, as shown in Fig. 19.1*d*. The load $2Q$ produces a bending moment that varies linearly along the span, from zero at the supports to maximum at midspan. Intuitively, one suspects that the best arrangement of prestressing would produce a *countermoment* that acts in the opposite sense to the load-induced moment and that would vary in the same way. This would be achieved by giving the tendon an eccentricity that varies linearly, from zero at the supports to maximum at midspan. This is shown in Fig. 19.1*d*. The stresses at midspan are the same as those in Fig. 19.1*c*, both when the load $2Q$ acts and when it does not. At the supports, where only the prestress force with zero eccentricity acts, a uniform compression stress f_c is obtained as shown.

For each characteristic load distribution, there is a *best tendon profile* that produces a prestress moment diagram that corresponds to that of the applied load. If the prestress countermoment is made exactly equal and opposite to the load-induced moment, the result is a beam that is subject only to uniform axial compressive stress in the concrete all along the span. Such a beam would be free of flexural cracking, and theoretically it would not be deflected up or down when that particular load is in place, compared to its position as originally cast. Such a result would be obtained for a load of $\frac{1}{2} \times 2Q = Q$, as shown in Fig. 19.1*e*, for example.

Some important conclusions can be drawn from these simple examples as follows:

1. Prestressing can control or even eliminate concrete tensile stress for specified loads.
2. Eccentric prestress is usually much more efficient than concentric prestress.
3. Variable eccentricity is usually preferable to constant eccentricity, from the viewpoints of both stress control and deflection control.

b. Equivalent Loads

The effect of a change in the vertical alignment of a prestressing tendon is to produce a vertical force on the concrete beam. That force, together with the prestressing force acting at the ends of the beam through the tendon anchorages, can be looked upon as a system of external loads.

In Fig. 19.2*a*, for example, a tendon that applies force P at the centroid of the concrete section at the ends of a beam and that has a uniform slope at angle $\cdot$ between the ends and midspan introduces a transverse force $2P \sin \cdot$ at the point of change of slope at midspan. At the anchorages, the vertical component of the prestressing force is $P \sin \cdot$ and the horizontal component is $P \cos \cdot$. The horizontal component is very nearly equal to P for the usual flat slope angles. The moment diagram for the beam of Fig. 19.2*a* is seen to have the same form as that for any center-loaded simple span.

The beam of Fig. 19.2*b*, with a curved tendon, is subject to a vertical upward load from the tendon as well as the forces P at each end. The exact distribution of the load depends on the profile of the tendon. A tendon with a parabolic profile, for example, will produce a uniformly distributed load. In this case, the moment diagram will be parabolic, as it is for a uniformly loaded simple span.

If a straight tendon is used with constant eccentricity, as shown in Fig. 19.2*c*, there are no vertical forces on the concrete, but the beam is subject to a moment Pe at each end, as well as the axial force P, and a diagram of constant moment results.

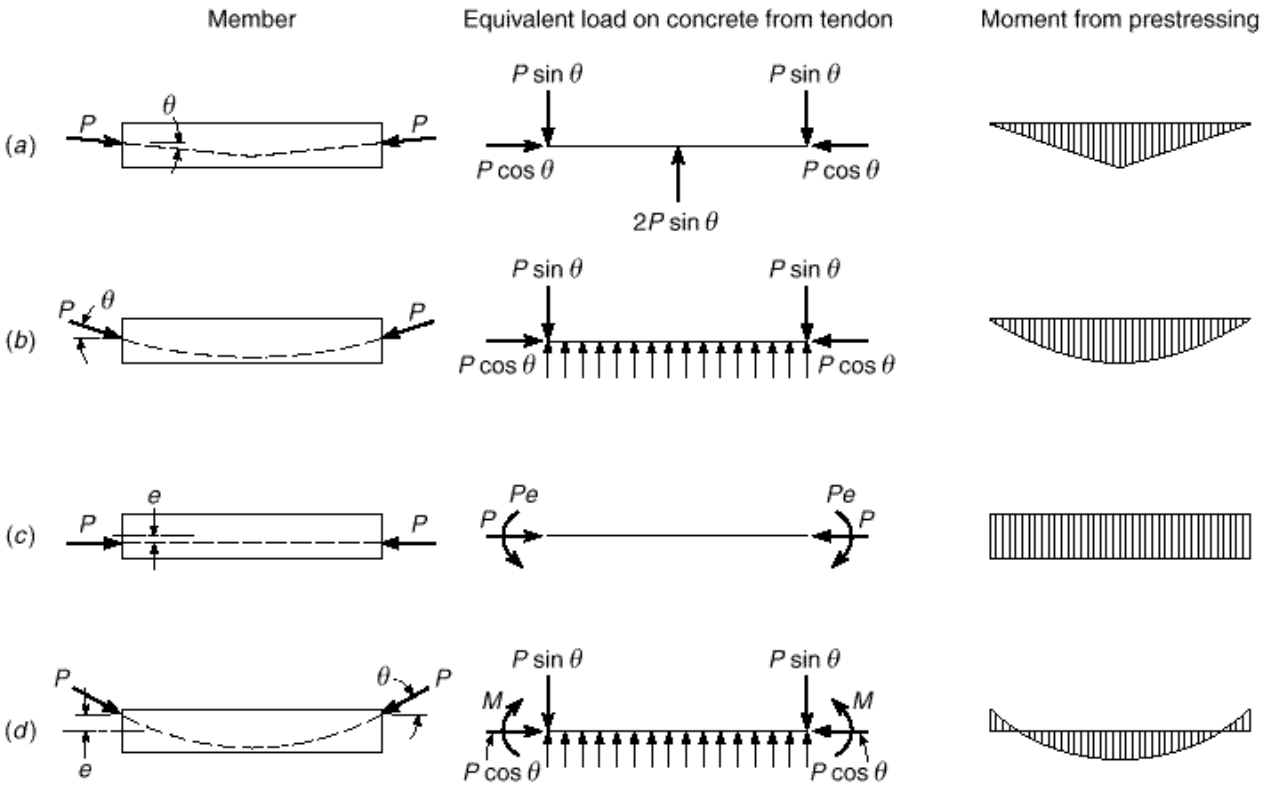

FIGURE 19.2
Equivalent loads and moments produced by prestressing tendons.

The end moment must also be accounted for in the beam shown in Fig. 19.2*d*, in which a parabolic tendon is used that does not pass through the concrete centroid at the ends of the span. In this case, a uniformly distributed upward load plus end anchorage forces are produced, as shown in Fig. 19.2*b*, but in addition, the end moments $M = Pe \cos \cdot$ must be accounted for.

It may be evident that for any arrangement of applied loads, a tendon profile can be selected so that the equivalent loads acting on the beam from the tendon are just equal and opposite to the applied loads. The result would be a state of pure compressive stress in the concrete, as discussed in somewhat different terms in reference to stress control and Fig. 19.1*e*. An advantage of the equivalent load concept is that it leads the designer to select what is probably the best tendon profile for a particular loading.

c. Prestressed Concrete as a Variation of Reinforced Concrete

In the descriptions of the effects of prestressing in Sections 19.2a and b, it was implied that the prestress force remained constant as the vertical load was introduced, that the concrete responded elastically, and that no concrete cracking occurred. These conditions may prevail up to about the service load level, but if the loads should be increased much beyond that, flexural tensile stresses will eventually exceed the modulus of rupture and cracks will form. Loads, however, can usually be increased much

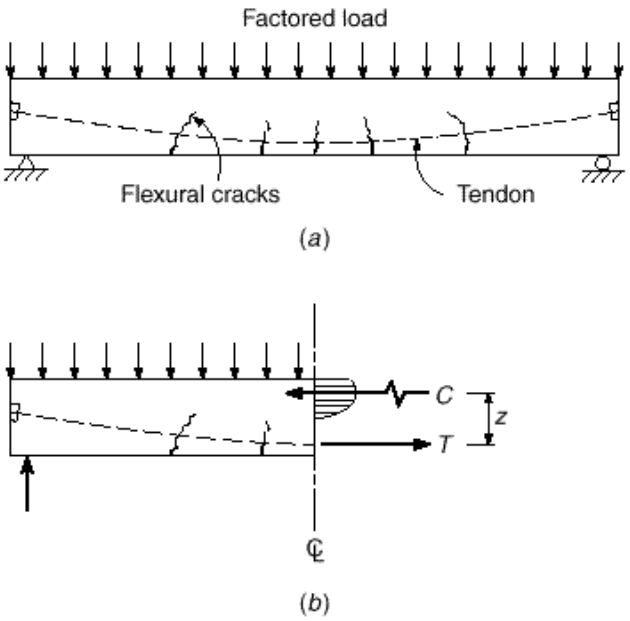

FIGURE 19.3
Prestressed concrete beam at load near flexural failure: (*a*) beam with factored load applied; (*b*) equilibrium of forces on left half of beam.

beyond the cracking load in well-designed prestressed beams, and depending on the level of prestress, the beam response at service load may vary from uncracked, to minor cracking, to fully cracked, as occurs for an ordinary reinforced concrete beam.

Eventually both the steel and concrete at the cracked section will be stressed into the inelastic range. The condition at incipient failure is shown in Fig. 19.3, which shows a beam carrying a *factored load* equal to some multiple of the expected service load. The beam undoubtedly would be in a partially cracked state; a possible pattern of flexural cracking is shown in Fig. 19.3*a*.

At the maximum moment section, only the concrete in compression is effective, and all of the tension is taken by the steel. The external moment from the applied loads is resisted by the internal force couple $Cz = Tz$. The behavior at this stage is almost identical to that of an ordinary reinforced concrete beam at overload. The main difference is that the very high strength steel used must be *prestrained* before loads are applied to the beam; otherwise, the high steel stresses would produce excessive concrete cracking and large beam deflections.

Each of the three viewpoints described—concrete stress control, equivalent loads, and reinforced concrete using prestrained steel—is useful in the analysis and design of prestressed concrete beams, and none of the three is sufficient in itself. Neither an elastic stress analysis nor an equivalent load analysis provides information about strength or safety margin. However, the stress analysis is helpful in predicting the extent of cracking, and the equivalent load analysis is often the best way to calculate deflections. Strength analysis is essential to evaluate safety against collapse, but it tells nothing about cracking or deflections of the beam under service conditions.

19.3 Sources of Prestress Force

Prestress can be applied to a concrete member in many ways. Perhaps the most obvious method of precompressing is to use jacks reacting against abutments, as shown in Fig. 19.4*a*. Such a scheme has been employed for large projects. Many variations are

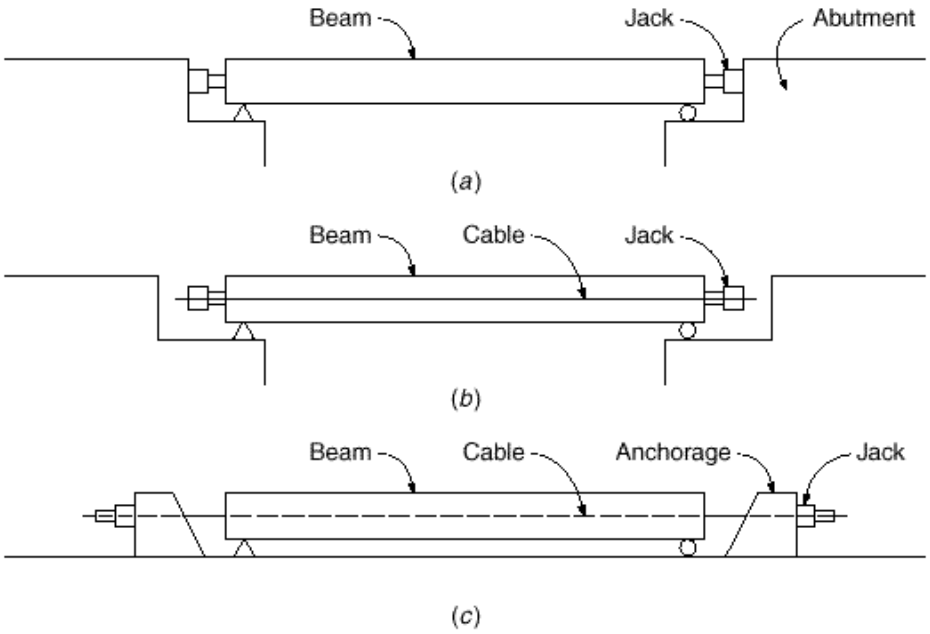

FIGURE 19.4
Prestressing methods: (*a*) post-tensioning by jacking against abutments; (*b*) post-tensioning with jacks reacting against beam; (*c*) pretensioning with tendon stressed between fixed external anchorages.

possible, including replacing the jacks with compression struts after the desired stress in the concrete is obtained or using inexpensive jacks that remain in place in the structure, in some cases with a cement grout used as the hydraulic fluid. The principal difficulty associated with such a system is that even a slight movement of the abutments will drastically reduce the prestress force.

In most cases, the same result is more conveniently obtained by tying the jack bases together with wires or cables, as shown in Fig. 19.4*b*. These wires or cables may be external, located on each side of the beam; more usually they are passed through a hollow conduit embedded in the concrete beam. Usually, one end of the prestressing tendon is anchored, and all of the force is applied at the other end. After reaching the desired prestress force, the tendon is wedged against the concrete and the jacking equipment is removed for reuse. In this type of prestressing, the entire system is self-contained and is independent of relative displacement of the supports.

Another method of prestressing that is widely used is illustrated by Fig. 19.4*c*. The prestressing strands are tensioned between massive abutments in a casting yard prior to placing the concrete in the beam forms. The concrete is placed around the tensioned strands, and after the concrete has attained sufficient strength, the jacking pressure is released. This transfers the prestressing force to the concrete by bond and friction along the strands, chiefly at the outer ends.

It is essential, in all three cases shown in Fig. 19.4, that the beam be supported in such a way as to permit the member to shorten axially without restraint so that the prestressing force can be transferred to the concrete.

Other means for introducing the desired prestressing force have been attempted on an experimental basis. Thermal prestressing can be achieved by preheating the steel by electrical or other means. Anchored against the ends of the concrete beam while in the extended state, the steel cools and tends to contract. The prestress force is developed through the restrained contraction. The use of expanding cement in concrete members has been tried with varying success. The volumetric expansion, restrained by steel strands or by fixed abutments, produces the prestress force.

FIGURE 19.5
Massive strand jacking abutment at the end of a long pretensioning bed. (*Courtesy of Concrete Technology Corporation.*)

Most of the patented systems for applying prestress in current use are variations of those shown in Fig. 19.4*b* and *c*. Such systems can generally be classified as *pretensioning* or *post-tensioning* systems. In the case of pretensioning, the tendons are stressed before the concrete is placed, as in Fig. 19.4*c*. This system is well suited for mass production, since casting beds can be made several hundred feet long, the entire length cast at once, and individual beams can be fabricated to the desired length in a single casting. Figure 19.5 shows workers using a hydraulic jack to tension strands at the anchorage of a long pretensioning bed. Although each tendon is individually stressed in this case, large capacity jacks are often used to tension all strands simultaneously.

In post-tensioned construction, shown in Fig. 19.4*b*, the tendons are tensioned after the concrete is placed and has gained its strength. Usually, a hollow conduit or sleeve is provided in the beam, through which the tendon is passed. In some cases, tendons are placed in the interior of hollow box-section beams. The jacking force is usually applied against the ends of the hardened concrete, eliminating the need for massive abutments. In Fig. 19.6, six tendons, each consisting of many individual strands, are being post-tensioned sequentially using a portable hydraulic jack.

A large number of particular systems, steel elements, jacks, and anchorage fittings have been developed in this country and abroad, many of which differ from each

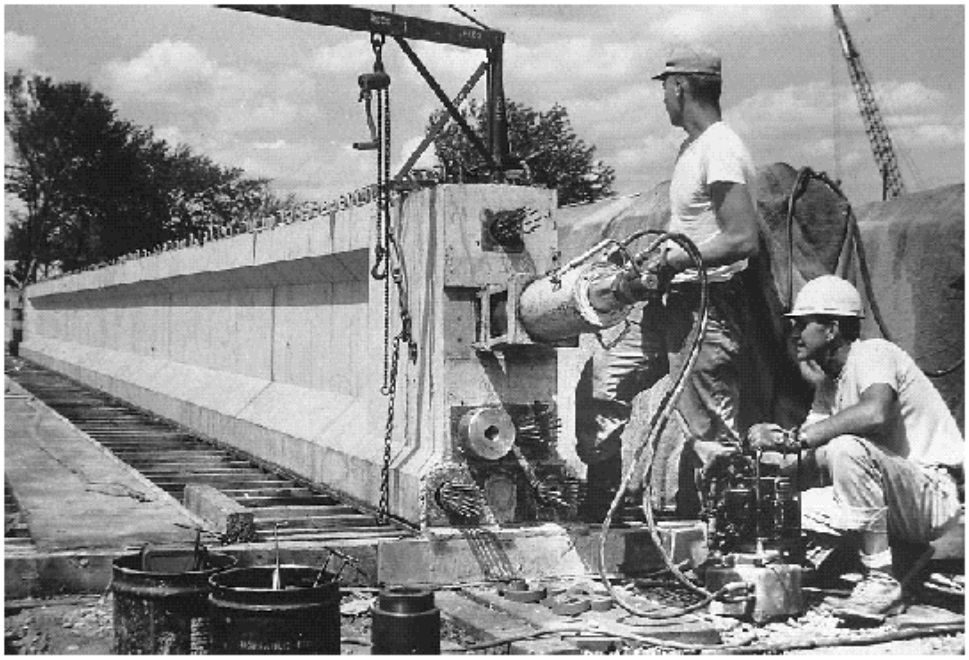

FIGURE 19.6
Post-tensioning a bridge girder using a portable jack to stress multistrand tendons. (*Courtesy of Concrete Technology Corporation.*)

other only in minor details (Refs. 19.1 to 19.8). As far as the designer of prestressed concrete structures is concerned, it is unnecessary and perhaps even undesirable to specify in detail the technique that is to be followed and the equipment to be used. It is frequently best to specify only the magnitude and line of action of the prestress force. The contractor is then free, in bidding the work, to receive quotations from several different prestressing subcontractors, with resultant cost savings. It is evident, however, that the designer must have some knowledge of the details of the various systems contemplated for use, so that in selecting cross-sectional dimensions, any one of several systems can be accommodated.

19.4 PRESTRESSING STEELS

Early attempts at prestressing concrete were unsuccessful because steel with ordinary structural strength was used. The low prestress obtainable in such rods was quickly lost due to shrinkage and creep in the concrete.

Such changes in length of concrete have much less effect on prestress force if that force is obtained using highly stressed steel wires or cables. In Fig. 19.7*a*, a concrete member of length L is prestressed using steel bars with ordinary strength stressed to 24,000 psi. With $E_s = 29 \times 10^6$ psi, the unit strain $\cdot_s$ required to produce the desired stress in the steel of 24,000 psi is

$$\cdot_s = \frac{\cdot L}{L} = \frac{f_s}{E_s} = \frac{24{,}000}{29 \times 10^6} = 8.0 \times 10^{-4}$$

However, the long-term strain in the concrete due to shrinkage and creep alone, if the prestress force were maintained over a long period, would be on the order of 8.0×10^{-4} and would be sufficient to completely relieve the steel of all stress.

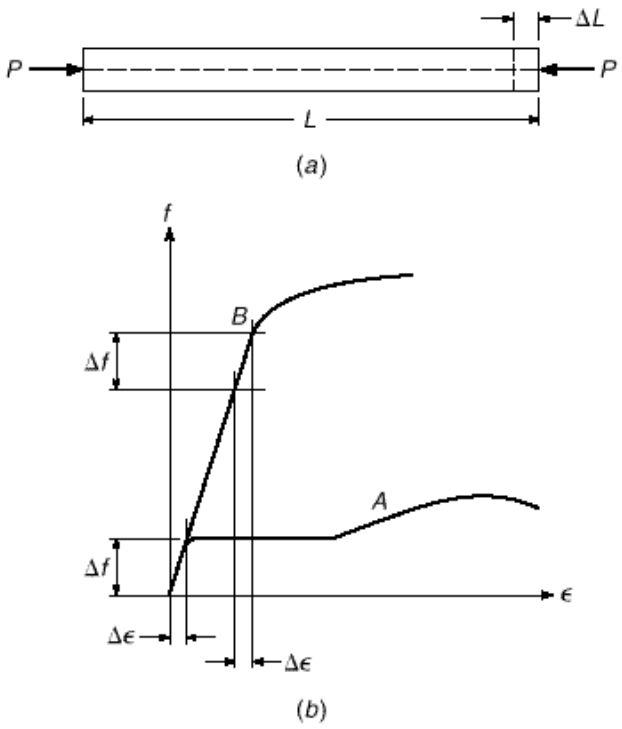

FIGURE 19.7
Loss of prestress due to concrete shrinkage and creep.

Alternatively, suppose that the beam is prestressed using high strength steel stressed to 150,000 psi. The elastic modulus of steel does not vary greatly, and the same value of 29×10^6 psi will be assumed here. Then in this case, the unit strain required to produce the desired stress in the steel is

$$\cdot_s = \frac{150{,}000}{29 \times 10^6} = 51.7 \times 10^{-4}$$

If shrinkage and creep strain are the same as before, the net strain in the steel after these losses is

$$\cdot_{s,net} = \cdot 51.7 - 8.0 \cdot \times 10^{-4} = 43.7 \times 10^{-4}$$

and the corresponding stress after losses is

$$f_s = \cdot_{s,net} E_s = \cdot 43.7 \times 10^{-4} \cdot \cdot 29 \times 10^6 \cdot = 127{,}000 \text{ psi}$$

This represents a stress loss of about 15 percent, compared with 100 percent loss in the beam using ordinary steel. It is apparent that the amount of stress lost because of shrinkage and creep is independent of the original stress in the steel. Therefore, the higher the original stress the lower the percentage loss. This is illustrated graphically by the stress-strain curves of Fig. 19.7*b*. Curve *A* is representative of ordinary reinforcing bars, with a yield stress of 60,000 psi, while curve *B* represents high tensile steel, with a tensile strength of 270,000 psi. The stress change Δf resulting from a certain change in strain $\Delta\cdot$ is seen to have much less effect when high steel stress levels are attained. Prestressing of concrete is therefore practical only when steels of very high strength are used.

Prestressing steel is most commonly used in the form of individual wires, stranded cable (strands) made up of seven wires, and alloy-steel bars. The physical

TABLE 19.1
Maximum permissible stresses in prestressing steel

1. Due to tendon jacking force but not greater than the lesser of $0.80f_{pu}$ and the maximum value recommended by the manufacturer of the prestressing steel or anchorage devices	$0.94f_{py}$
2. Immediately after prestress transfer but not greater than $0.74f_{pu}$	$0.82f_{py}$
3. Post-tensioning tendons, at anchorage devices and couplers, immediately after tendon anchorage	$0.70f_{pu}$

properties of these have been discussed in Section 2.16, and typical stress-strain curves appear in Fig. 2.16. Virtually all strands in use are low-relaxation (Section 2.16c).

The tensile stress permitted by ACI Code 18.5 in prestressing wires, strands, or bars is dependent upon the stage of loading. When the jacking force is first applied, a maximum stress of $0.80\,f_{pu}$ or $0.94\,f_{py}$ is allowed, whichever is smaller, where f_{pu} is the tensile strength of the steel and f_{py} is the yield strength. Immediately after transfer of prestress force to the concrete, the permissible stress is $0.74\,f_{pu}$ or $0.82\,f_{py}$, whichever is smaller (except at post-tensioning anchorages where the stress is limited to $0.70\,f_{pu}$). The justification for a higher allowable stress during the stretching operation is that the steel stress is known quite precisely at this stage. Hydraulic jacking pressure and total steel strain are quantities that are easily measured and quality control specifications require correlation of load and deflection at jacking (Ref. 19.9). In addition, if an accidentally deficient tendon should break, it can be replaced; in effect, the tensioning operation is a performance test of the material. The lower values of allowable stress apply after elastic shortening of the concrete, frictional loss, and anchorage slip have taken place. The steel stress is further reduced during the life of the member due to shrinkage and creep in the concrete and relaxation in the steel. ACI allowable stresses in prestressing steels are summarized in Table 19.1.

The strength and other characteristics of prestressing wire, strands, and bars vary somewhat between manufacturers, as do methods of grouping tendons and anchoring them. Typical information is given for illustration in Table A.15 of Appendix A and in Refs. 19.1 to 19.8.

19.5 Concrete for Prestressed Construction

Ordinarily, concrete of substantially higher compressive strength is used for prestressed structures than for those constructed of ordinary reinforced concrete. Most prestressed construction in the United States at present is designed for a compressive strength above 5000 psi. There are several reasons for this:

1. High-strength concrete normally has a higher modulus of elasticity (see Fig. 2.3). This means a reduction in initial elastic strain under application of prestress force and a reduction in creep strain, which is approximately proportional to elastic strain. This results in a reduction in loss of prestress.
2. In post-tensioned construction, high bearing stresses result at the ends of beams where the prestressing force is transferred from the tendons to anchorage fittings, which bear directly against the concrete. This problem can be met by increasing the

TABLE 19.2
Permissible stresses in concrete in prestressed flexural members

	Class		
Condition†	U	T	C*
a. Extreme fiber stress in compression immediately after transfer	$0.60f_{ci}$	$0.60f_{ci}$	$0.60f_{ci}$
b. Extreme fiber stress in tension immediately after transfer (except as in c)†	$3\sqrt{f'_{ci}}$	$3\sqrt{f'_{ci}}$	$3\sqrt{f'_{ci}}$
c. Extreme fiber stress in tension immediately after transfer at the end of a simply supported member‡	$6\sqrt{f'_{ci}}$	$6\sqrt{f'_{ci}}$	$6\sqrt{f'_{ci}}$
d. Extreme fiber stress in compression due to prestress plus sustained load	$0.45f'_c$	$0.45f'_c$	—
e. Extreme fiber stress in compression due to prestress plus total load	$0.60f'_c$	$0.60f'_c$	—
f. Extreme fiber stress in tension f_t in precompressed tensile zone under service load	$\leq 7.5\sqrt{f'_c}$	$> 7.5\sqrt{f'_c}$ and $\leq 12\sqrt{f'_c}$	—

* There are no service stress requirements for Class C.

† Permissible stresses may be exceeded if it is shown by test or analysis that performance will not be impaired.

‡ When computed tensile stresses exceed these values, bonded auxiliary prestressed or nonprestressed reinforcement shall be provided in the tensile zone to resist the total tensile force in the concrete computed with the assumption of an uncracked section.

size of the anchorage fitting or by increasing the bearing capacity of the concrete by increasing its compressive strength. The latter is usually more economical.

3. In pretensioned construction, where transfer by bond is customary, the use of high-strength concrete will permit the development of higher bond stresses.
4. A substantial part of the prestressed construction in the United States is precast, with the concrete mixed, placed, and cured under carefully controlled conditions that facilitate obtaining higher strengths.

The strain characteristics of concrete under short-term and sustained loads assume an even greater importance in prestressed structures than in reinforced concrete structures because of the influence of strain on loss of prestress force. Strains due to stress, together with volume changes due to shrinkage and temperature changes, may have considerable influence on prestressed structures. In this connection, it is suggested that the reader review Sections 2.8 to 2.11, which discuss in some detail the compressive and tensile strengths of concrete under short-term and sustained loads and the changes in concrete volume that occur due to shrinkage and temperature change.

As for prestressing steels, the allowable stresses in the concrete, according to ACI Code 18.4, depend upon the stage of loading and the behavior expected of the member. ACI Code 18.3.3 defines three classifications of behavior, depending on the extreme fiber stress f_t at service load in the precompressed tensile zone. The three clas-

sufficient period of time to cause significant time-dependent deflections, whereas *total load* refers to the total service load, a part of which may be transient or temporary live load. Thus, sustained load would include dead load and may or may not include service live load, depending on its duration. If the live load duration is short or intermittent, the higher limit of part e is permitted.

Two-way slabs are designated as Class U flexural members.† Class C flexural members have no service level stress requirements but must satisfy strength and serviceability requirements. Service load stress calculations are computed based on uncracked section properties for Class U and T flexural members and on the cracked section properties for Class C members.

19.6 Elastic Flexural Analysis

It has been noted earlier in this text that the design of concrete structures may be based either on providing sufficient strength, which would be used fully only if the expected loads were increased by an overload factor, or on keeping material stresses within permissible limits when actual service loads act. In the case of ordinary reinforced concrete members, strength design is used. Members are proportioned on the basis of strength requirements and then checked for satisfactory service load behavior, notably with respect to deflection and cracking. The design is then modified if necessary.

Class C members are principally designed based on strength. Class U and T members, however, are proportioned so that stresses in the concrete and steel at actual service loads are within permissible limits. These limits are a fractional part of the actual capacities of the materials. There is some logic to this approach, since an important objective of prestressing is to improve the performance of members at service loads. Consequently, service load requirements often control the amount of prestress force used in Class U and Class T members. Design based on service loads may usually be carried out assuming elastic behavior of both the concrete and the steel, since stresses are relatively low in each.

Regardless of the starting point chosen for the design, a structural member must be satisfactory at all stages of its loading history. Accordingly, prestressed members proportioned on the basis of permissible stresses must also be checked to ensure that sufficient strength is provided should overloads occur, and deflection and cracking under service loads should be investigated. Consistent with most U.S. practice, in this text the design of prestressed concrete beams will start with a consideration of stress limits, after which strength and other properties will be checked.

It is convenient to think of prestressing forces as a system of external forces acting on a concrete member, which must be in equilibrium under the action of those forces. Figure 19.8*a* shows a simple-span prestressed beam with curved tendons, typical of many post-tensioned members. The portion of the beam to the left of a vertical cutting plane *x-x* is taken as a free body, with forces acting as shown in Fig. 19.8*b*. The force P at the left end is exerted on the concrete through the tendon anchorage, while the force P at the cutting plane *x-x* results from combined shear and normal stresses acting at the concrete surface at that location. The direction of P is tangent to the curve of the tendon at each location. Note the presence of the force N, acting on the concrete from the tendon, due to tendon curvature. This force will be distributed in some man-

† While the ACI Code allows up to $7.5\cdot\sqrt{f'_c}$ as the maximum tensile stress in the precompressed tensile zone of uncracked members, research and design practice for two-way slabs has limited the maximum tensile stress to $6\cdot\sqrt{f'_c}$.

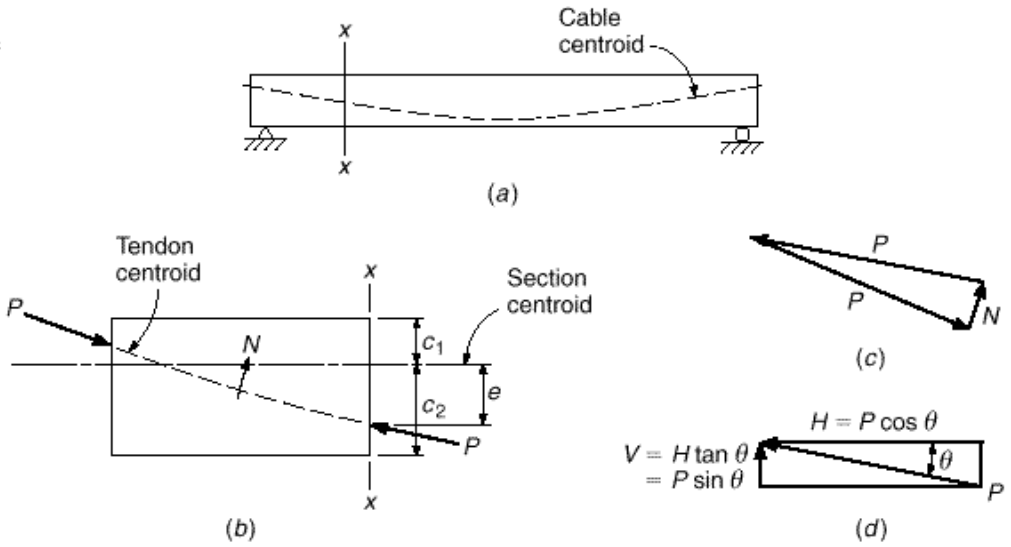

FIGURE 19.8
Prestressing forces acting on concrete.

ner along the length of the tendon, the exact distribution depending upon the tendon profile. Its resultant and the direction in which the resultant acts can be found from the force diagram of Fig. 19.8*c*.

It is convenient when working with the prestressing force P to divide it into its components in the horizontal and vertical directions. The horizontal component (Fig. 19.8*d*) is $H = P \cos \cdot$, and the vertical component is $V = H \tan \cdot = P \sin \cdot$, where $\cdot$ is the angle of inclination of the tendon centroid at the particular section. Since the slope angle is normally quite small, the cosine of $\cdot$ is very close to unity and it is sufficient for most calculations to take $H = P$.

The magnitude of the prestress force is not constant. The *jacking force* P_j is immediately reduced to what is termed the *initial prestress force* P_i because of elastic shortening of the concrete upon transfer, slip of the tendon as the force is transferred from the jacks to the beam ends, and loss due to friction between the tendon and the concrete (post-tensioning) or between the tendon and cable alignment devices (pretensioning). There is a further reduction of force from P_i to the *effective prestress* P_e, occurring over a long period of time at a gradually decreasing rate, because of concrete creep under the sustained prestress force, concrete shrinkage, and relaxation of stress in the steel. Methods for predicting losses will be discussed in Section 19.13. Of primary interest to the designer are the initial prestress P_i immediately after transfer and the final or effective prestress P_e after all losses.

In developing elastic equations for flexural stress, the effects of prestress force, self-weight moment, and dead and live load moments are calculated separately, and the separate stresses are superimposed. When the initial prestress force P_i is applied with an eccentricity e below the centroid of the cross section with area A_c and top and bottom fiber distances c_1 and c_2, respectively, it causes the compressive stress $-P_i \cdot A_c$ and the bending stresses $+P_i e c_1 \cdot I_c$ and $-P_i e c_2 \cdot I_c$ in the top and bottom fibers, respectively (compressive stresses are designated as negative, tensile stresses as positive), as shown in Fig. 19.9*a*. Then, at the top fiber, the stress is

$$f_1 = -\frac{P_i}{A_c} + \frac{P_i e c_1}{I_c} = -\frac{P_i}{A_c} \cdot 1 - \frac{e c_1}{r^2} \cdot \qquad (19.1a)$$

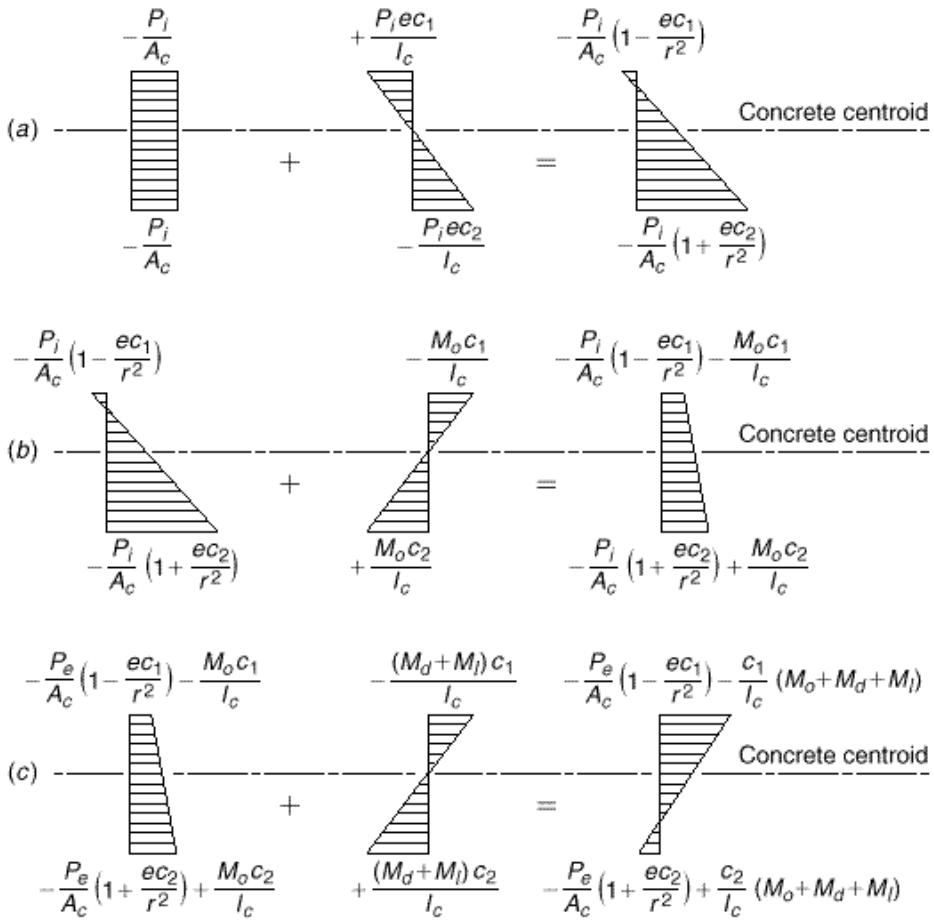

FIGURE 19.9
Concrete stress distributions in beams: (*a*) effect of prestress; (*b*) effect of prestress plus self-weight of beam; (*c*) effect of prestress, self-weight, and external dead and live service loads.

and at the bottom fiber

$$f_2 = -\frac{P_i}{A_c} - \frac{P_i e c_2}{I_c} = -\frac{P_i}{A_c}\cdot\left(1 + \frac{e c_2}{r^2}\right) \tag{19.1b}$$

where r is the radius of gyration of the concrete section. Normally, as the eccentric prestress force is applied, the beam deflects upward. The beam self-weight w_o then causes additional moment M_o to act, and the net top and bottom fiber stresses become

$$f_1 = -\frac{P_i}{A_c}\cdot\left(1 - \frac{e c_1}{r^2}\right) - \frac{M_o c_1}{I_c} \tag{19.2a}$$

$$f_2 = -\frac{P_i}{A_c}\cdot\left(1 + \frac{e c_2}{r^2}\right) + \frac{M_o c_2}{I_c} \tag{19.2b}$$

as shown in Fig. 19.9*b*. At this stage, time-dependent losses due to shrinkage, creep, and relaxation commence, and the prestressing force gradually decreases from P_i to P_e. It is usually acceptable to assume that all such losses occur prior to the application of service loads, since the concrete stresses at service loads will be critical after losses, not before. Accordingly, the stresses in the top and bottom fiber, with P_e and beam load acting, become

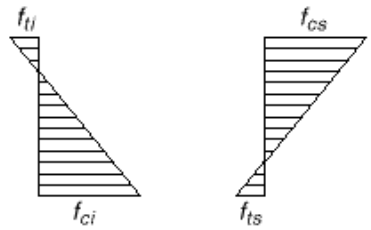

FIGURE 19.10
Stress limits: (*a*) unloaded beam, with initial prestress plus self-weight; (*b*) loaded beam, with effective prestress, self-weight, and full service load.

$$f_1 = -\frac{P_e}{A_c}\left(1 - \frac{ec_1}{r^2}\right) - \frac{M_o c_1}{I_c} \tag{19.3a}$$

$$f_2 = -\frac{P_e}{A_c}\left(1 + \frac{ec_2}{r^2}\right) + \frac{M_o c_2}{I_c} \tag{19.3b}$$

When full service loads (dead load in addition to self-weight of the beam, plus service live load) are applied, the stresses are

$$f_1 = -\frac{P_e}{A_c}\left(1 - \frac{ec_1}{r^2}\right) - \frac{(M_o + M_d + M_l)c_1}{I_c} \tag{19.4a}$$

$$f_2 = -\frac{P_e}{A_c}\left(1 + \frac{ec_2}{r^2}\right) + \frac{(M_o + M_d + M_l)c_2}{I_c} \tag{19.4b}$$

as shown in Fig. 19.9*c*.

It is necessary, in reviewing the adequacy of a beam (or in designing a beam on the basis of permissible stresses), that the stresses in the extreme fibers remain within specified limits under any combination of loadings that can occur. Normally, the stresses at the section of maximum moment, in a properly designed beam, must stay within the limit states defined by the distributions shown in Fig. 19.10 as the beam passes from the unloaded stage (P_i plus self-weight) to the loaded stage (P_e plus full service loads). In the figure, f_{ci} and f_{ti} are the permissible compressive and tensile stresses, respectively, in the concrete immediately after transfer, and f_{cs} and f_{ts} are the permissible compressive and tensile stresses at service loads (see Table 19.2).

In calculating the section properties A_c, I_c, etc., to be used in the above equations, it is relevant that, in post-tensioned construction, the tendons are usually grouted in the conduits after tensioning. Before grouting, stresses should be based on the net section with holes deducted. After grouting, the transformed section should be used with holes considered filled with concrete and with the steel replaced with an equivalent area of concrete. However, it is satisfactory, unless the holes are quite large, to compute section properties on the basis of the gross concrete section. Similarly, while in pretensioned beams the properties of the transformed section should be used, it makes little difference if calculations are based on properties of the gross concrete section.[†]

[†] ACI Code 18.2.6 contains the following provision: "In computing section properties prior to bonding of prestressing steel, the effect of loss of area due to open ducts shall be considered." It is noted in ACI Commentary 18.2.6 that "If the effect of the open duct area on design is deemed negligible, section properties may be based on total area. In post-tensioned members after grouting and in pretensioned members, section properties may be based on effective sections using transformed areas of bonded prestressing steel and nonprestressed gross sections, or net sections."

FIGURE 19.11
Location of kern points.

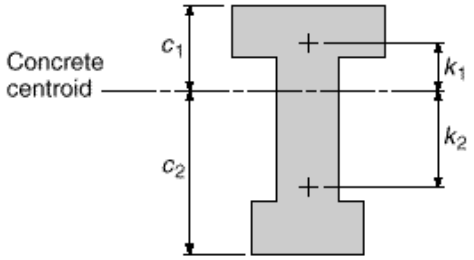

It is useful to establish the location of the upper and lower *kern points* of a cross section. These are defined as the limiting points inside which the prestress force resultant may be applied without causing tension anywhere in the cross section. Their locations are obtained by writing the expression for the tensile fiber stress due to application of an eccentric prestress force acting alone and setting this expression equal to zero to solve for the required eccentricity. In Fig. 19.11, to locate the upper kern-point distance k_1 from the neutral axis, let the prestress force resultant P act at that point. Then the bottom fiber stress is

$$f_2 = -\frac{P}{A_c}\cdot\left(1 + \frac{ec_2}{r^2}\right) = 0$$

Thus, with

$$1 + \frac{ec_2}{r^2} = 0$$

one obtains the corresponding eccentricity

$$e = k_1 = -\frac{r^2}{c_2} \tag{19.5a}$$

Similarly, the lower kern-point distance k_2 is

$$k_2 = \frac{r^2}{c_1} \tag{19.5b}$$

The region between these two limiting points is known as the *kern*, or in some cases the *core*, of the section.

EXAMPLE 19.1

Pretensioned I beam with constant eccentricity. A simply supported symmetrical I beam shown in cross section in Fig. 19.12*a* will be used on a 40 ft simple span. It has the following section properties:

Moment of inertia:	I_c	$= 12{,}000\ \text{in}^4$
Concrete area:	A_c	$= 176\ \text{in}^2$
Radius of gyration:	r^2	$= 68.2\ \text{in}^2$
Section modulus:	S	$= 1000\ \text{in}^3$
Self-weight:	w_o	$= 0.183$ kips·ft

and is to carry a superimposed dead plus live load (considered "sustained," not short-term) of 0.750 kips/ft in addition to its own weight. The beam will be pretensioned with multiple seven-wire strands with the centroid at a constant eccentricity of 7.91 in. The prestress force P_i immediately after transfer will be 158 kips; after time-dependent losses, the force will reduce to $P_e = 134$ kips. The specified strength of the concrete $f'_c = 5000$ psi, and at the time of prestressing the strength will be $f'_{ci} = 3750$ psi. Calculate the concrete flexural stresses at

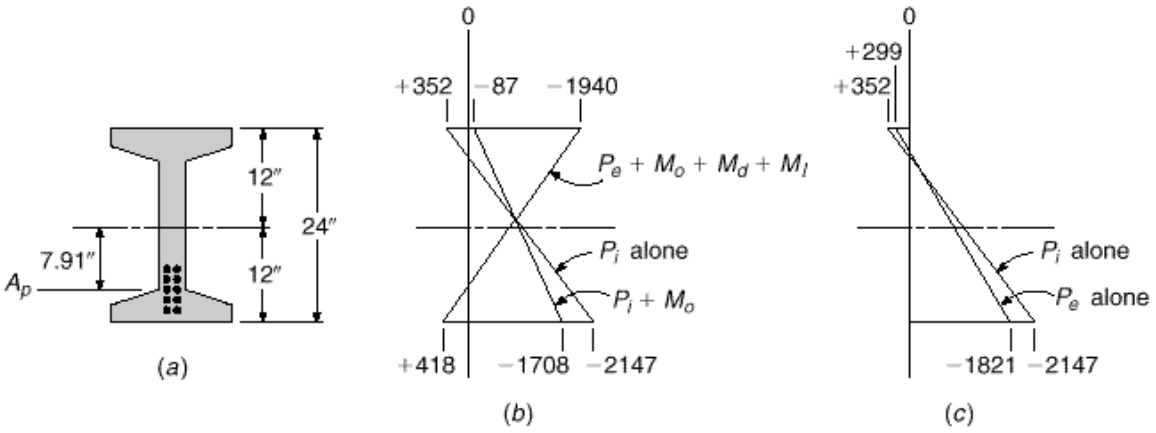

FIGURE 19.12
Pretensioned I beam. Design example: (*a*) cross section, (*b*) stresses at midspan (psi), (*c*) stresses at ends (psi).

the midspan section of the beam at the time of transfer, and after all losses with full service load in place. Compare with ACI allowable stresses for a Class U member.

SOLUTION. Stresses in the concrete resulting from the initial prestress force of 158 kips may be found by Eqs. (19.1*a*) and (19.1*b*):

$$f_1 = -\frac{158{,}000}{176} \cdot 1 - \frac{7.91 \times 12}{68.2} \cdot = +352 \text{ psi}$$

$$f_2 = -\frac{158{,}000}{176} \cdot 1 + \frac{7.91 \times 12}{68.2} \cdot = -2147 \text{ psi}$$

The self-weight of the beam causes the immediate superposition of a moment of

$$M_o = 0.183 \times \frac{40^2}{8} = 36.6 \text{ ft-kips}$$

and corresponding stresses of $36{,}600 \times 12 \cdot 1000 = 439$ psi, so that the net stresses at the top and bottom of the concrete section due to initial prestress and self-weight, from Eqs. (19.2*a*) and (19.2*b*), are

$$f_1 = +352 - 439 = -87 \text{ psi}$$

$$f_2 = -2147 + 439 = -1708 \text{ psi}$$

After losses, the prestress force is reduced to 134 kips, and the concrete stresses due to that force plus self-weight are

$$f_1 = +352 \times \frac{134}{158} - 439 = 140 \text{ psi}$$

$$f_2 = -2147 \times \frac{134}{158} + 439 = -1382 \text{ psi}$$

and stresses at the end of the beam are

$$f_1 = +352 \cdot \frac{134}{158} \cdot = 299$$

$$f_2 = -2147 \cdot \frac{134}{158} \cdot = 1821$$

The superimposed load of 0.750 kips/ft produces a midspan moment of $M_d + M_l = 0.750 \times 40^2 \cdot 8 = 150$ ft-kips, and the corresponding stresses of $150{,}000 \times 12 \cdot 1000 = 1800$ psi in compression and tension at the top and bottom of the beam, respectively. Thus, the service load stresses at the top and bottom faces are

$$f_1 = -140 - 1800 = -1940 \text{ psi}$$

$$f_2 = -1382 + 1800 = +418 \text{ psi}$$

Concrete stresses at midspan are shown in Fig. 19.12*b* and at the beam end in Fig. 19.12*c*. According to the ACI Code (see Table 19.2), the stresses permitted in the concrete are

$$\text{Tension at transfer: } f_{ti} = 3 \cdot \sqrt{3750} = +184 \text{ psi}$$

$$\text{Compression at transfer: } f_{ci} = 0.60 \times 3750 = -2250 \text{ psi}$$

$$\text{Tension at service load: } f_{ts} = 7.5 \cdot \sqrt{5000} = +530 \text{ psi}$$

$$\text{Compression at service load: } f_{cs} = 0.45 \times 5000 = -2250 \text{ psi}$$

At the initial stage, with prestress plus self-weight in place, the actual compressive stress of 1708 psi is well below the limit of 2250 psi, and no tension acts at the top, although 184 psi is allowed. While more prestress force or more eccentricity might be suggested to more fully utilize the section, to attempt to do so in this beam, with constant eccentricity, would violate limits at the support, where self-weight moment is zero. It is apparent that at the supports, the initial prestress force acting alone produces tension of 352 psi at the top of the beam (Fig. 19.12*c*), barely below the permitted value of $6 \cdot \sqrt{3750} = 367$, so very little improvement can be made. Finally, at full service load, the tension of 418 psi is under the allowed 530 psi, and compression of 1940 psi is well below the permitted 2250 psi.

19.7 Flexural Strength

In an ordinary reinforced concrete beam, the stress in the tensile steel and the compressive force in the concrete increase in proportion to the applied moment up to and somewhat beyond service load, with the distance between the two internal stress resultants remaining essentially constant. In contrast to this behavior, in a prestressed beam, increased moment is resisted by a proportionate increase in the distance between the compressive and tensile resultant forces, the compressive resultant moving upward as the load is increased. The magnitude of the internal forces remains nearly constant up to, and usually somewhat beyond, service loads.

This situation changes drastically upon flexural tensile cracking of the prestressed beam. When the concrete cracks, there is a sudden increase in the stress in the steel as the tension that was formerly carried by the concrete is transferred to it. After cracking, the prestressed beam behaves essentially like an ordinary reinforced concrete beam. The compressive resultant cannot continue to move upward indefinitely, and increasing moment must be accompanied by a nearly proportionate increase in steel stress and compressive force. The strength of a prestressed beam can, therefore, be predicted by the same methods developed for ordinary reinforced concrete beams, with modifications to account for (a) the different shape of the stress-strain curve for prestressing steel, as compared with that for ordinary reinforcement, and (b) the tensile strain already present in the prestressing steel before the beam is loaded.

Highly accurate predictions of the flexural strength of prestressed beams can be made based on a *strain compatibility analysis* that accounts for these factors in a rational and explicit way (Ref. 19.1). For ordinary design purposes, certain approxi-

mate relationships have been derived. ACI Code 18.7 and the accompanying ACI Commentary 18.7 include approximate equations for flexural strength that will be summarized in the following paragraphs.

a. Stress in the Prestressed Steel at Flexural Failure

When a prestressed concrete beam fails in flexure, the prestressing steel is at a stress f_{ps} that is higher than the effective prestress f_{pe} but below the tensile strength f_{pu}. If the effective prestress $f_{pe} = P_e / A_{ps}$ is not less than $0.50 f_{pu}$, ACI Code 18.7.2 permits use of certain approximate equations for f_{ps}. These equations appear quite complex as they are presented in the ACI Code, mainly because they are written in general form to account for differences in type of prestressing steel and to apply to beams in which nonprestressed bar reinforcement may be included in the flexural tension zone or the compression region or both. Separate equations are given for members with bonded tendons and unbonded tendons because, in the latter case, the increase in steel stress at the maximum moment section as the beam is overloaded is much less than if the steel were bonded throughout its length.

For the basic case, in which the prestressed steel provides all of the flexural reinforcement, the ACI Code equations can be stated in simplified form as follows:

1. For members with bonded tendons:

$$f_{ps} = f_{pu}\left(1 - \frac{\rho_p}{\beta_1}\frac{\rho_p f_{pu}}{f'_c}\right) \tag{19.6}$$

where $\rho_p = A_{ps}/bd_p$, d_p = effective depth to the prestressing steel centroid, b = width of compression face, β_1 = the familiar relations between stress block depth and depth to the neutral axis [Eq. (3.26)], and γ_p is a factor that depends on the type of prestressing steel used, as follows:

$$\gamma_p = \begin{cases} 0.55 \text{ for } f_{py}/f_{pu} \geq 0.80 & \text{(typical high-strength bars)} \\ 0.40 \text{ for } f_{py}/f_{pu} \geq 0.85 & \text{(typical ordinary strand)} \\ 0.28 \text{ for } f_{py}/f_{pu} \geq 0.90 & \text{(typical low-relaxation strand)} \end{cases}$$

2. For members with unbonded tendons and with a span-depth ratio of 35 or less (this includes most beams),

$$f_{ps} = f_{pe} + 10{,}000 + \frac{f'_c}{100\rho_p} \tag{19.7}$$

but not greater than f_{py} and not greater than $f_{pe} + 60{,}000$ psi.

3. For members with unbonded tendons and with span-depth ratio greater than 35 (applying to many slabs),

$$f_{ps} = f_{pe} + 10{,}000 + \frac{f'_c}{300\rho_p} \tag{19.8}$$

but not greater than f_{py} and not greater than $f_{pe} + 30{,}000$ psi.

b. Nominal Flexural Strength and Design Strength

With the stress in the prestressed tensile steel when the member fails in flexure established by Eq. (19.6), (19.7), or (19.8), the nominal flexural strength can be calculated

by methods and equations that correspond directly with those used for ordinary reinforced concrete beams. For rectangular cross sections, or flanged sections such as I or T beams in which the stress block depth is equal to or less than the average flange thickness, the nominal flexural strength is

$$M_n = A_{ps} f_{ps} \cdot d_p - \frac{a}{2} \cdot \tag{19.9}$$

where

$$a = \frac{A_{ps} f_{ps}}{0.85 f_c' b} \tag{19.10}$$

Equations (19.9) and (19.10) can be combined as follows:

$$M_n = \cdot \, _p f_{ps} b d_p^2 \cdot 1 - 0.588 \frac{\cdot \, _p f_{ps}}{f_c'} \cdot \tag{19.11}$$

In all cases, the *flexural design strength* is taken equal to $\cdot \, M_n$, where $\cdot$ is the strength reduction factor for flexure (see Section 19.7c).

If the stress block depth exceeds the average flange thickness, the method for calculating flexural strength is exactly analogous to that used for ordinary reinforced concrete I and T beams. The total prestressed tensile steel area is divided into two parts for computational purposes. The first part A_{pf}, acting at the stress f_{ps}, provides a tensile force to balance the compression in the overhanging parts of the flange. Thus,

$$A_{pf} = 0.85 \frac{f_c'}{f_{ps}} \cdot b - b_w \cdot h_f \tag{19.12}$$

The remaining prestressed steel area

$$A_{pw} = A_{ps} - A_{pf} \tag{19.13}$$

provides tension to balance the compression in the web. The total resisting moment is the sum of the contributions of the two force couples:

$$M_n = A_{pw} f_{ps} \cdot d_p - \frac{a}{2} \cdot + A_{pf} f_{ps} \cdot d_p - \frac{h_f}{2} \cdot \tag{19.14a}$$

or

$$M_n = A_{pw} f_{ps} \cdot d_p - \frac{a}{2} \cdot + 0.85 f_c' \cdot b - b_w \cdot h_f \cdot d_p - \frac{h_f}{2} \cdot \tag{19.14b}$$

where

$$a = \frac{A_{pw} f_{ps}}{0.85 f_c' b_w} \tag{19.15}$$

As before, the design strength is taken as $\cdot \, M_n$, where $\cdot$ is typically 0.90, as discussed in Section 19.7c.

If, after a prestressed beam is designed by elastic methods at service loads, it has inadequate strength to provide the required safety margin under factored load, nonprestressed reinforcement can be added on the tension side and will work in combination with the prestressing steel to provide the needed strength. Such nonprestressed steel, with area A_s, can be assumed to act at its yield stress f_y, to contribute a tension

force at the nominal moment of $A_s f_y$. The reader should consult ACI Code 18.7 and ACI Commentary 18.7 for equations for prestressed steel stress at failure and for flexural strength, which are direct extensions of those given above.

c. Limits for Reinforcement

The ACI Code classifies prestressed concrete flexural members as tension-controlled or compression-controlled based on the net tensile strain ε_t in the same manner as done for ordinary reinforced concrete beams. Section 3.4d describes the strain distributions and the variation of strength-reduction factors associated with limitations on the net tensile strain. Recall that the net tensile strain excludes strains due to creep, shrinkage, temperature, and effective prestress. To maintain a strength-reduction factor ϕ of 0.90 and ensure that, if flexural failure were to occur, it would be a ductile failure, a net tensile strain of at least 0.005 is required. Due to the complexity of computing net tensile strain in prestressed members, it is easier to perform the check using the c/d_t ratio. From Fig. 3.10a, this simplifies to

$$\frac{c}{d_t} \leq 0.375 \tag{19.16}$$

where d_t is the distance from the extreme compressive fiber to the extreme tensile steel. In many cases, d_t will be the same as d_p, the distance from the extreme compressive fiber to the centroid of the prestressed reinforcement. However, when supplemental nonprestressed steel is used or the prestressing strands are distributed through the depth of the section, d_t will be greater than d_p. If the prestressed beam does not meet the requirements of Eq. (19.16), it may no longer be considered as tension-controlled, and the strength reduction factor ϕ must be determined as shown in Fig. 3.9. If $c/d_t \geq 0.60$, corresponding to $\varepsilon_t \leq 0.002$, the section is considered to be *over-reinforced*, and alternative equations must be derived for computing the flexural strength (see Ref. 19.1).

It will be recalled that a *minimum tensile reinforcement ratio* is required for ordinary reinforced concrete beams, so that the beams will be safe from sudden failure upon the formation of flexural cracks. For prestressed beams, because of the same concern, ACI Code 18.8.2 requires that the total tensile reinforcement must be adequate to support a factored load of at least 1.2 times the cracking load of the beam, calculated on the basis of a modulus of rupture of $7.5\sqrt{f'_c}$.

d. Minimum Bonded Reinforcement

To control cracking in beams and one-way prestressed slabs with *unbonded tendons*, some bonded reinforcement must be added in the form of nonprestressed reinforcing bars, uniformly distributed over the tension zone as close as permissible to the extreme tension fiber. According to ACI Code 18.9.2, the minimum amount of such reinforcement is

$$A_s = 0.004A \tag{19.17}$$

where A is the area of that part of the cross section between the flexural tension face and the centroid of the gross concrete cross section. Exceptions are provided for two-way slabs with very low tensile stresses.

EXAMPLE 19.2 **Flexural strength of pretensioned I beam.** The prestressed I beam shown in cross section in Fig. 19.13 is pretensioned using five low relaxation stress-relieved Grade 270 $\frac{1}{2}$ in. diameter strands, carrying effective prestress $f_{pe} = 160$ ksi. Concrete strength is $f'_c = 4000$ psi. Calculate the design strength of the beam.

SOLUTION. The effective prestress in the strands of 160 ksi is well above $0.50 \times 270 = 135$ ksi, confirming that the approximate ACI equations are applicable. The tensile reinforcement ratio is

$$\rho_p = \frac{0.765}{12 \times 17.19} = 0.0037$$

and the steel stress f_{ps} when the beam fails in flexure is found from Eq. (19.6) to be

$$f_{ps} = 270 \cdot 1 - \frac{0.28}{0.85} \frac{0.0037 \times 270}{4} \cdot = 248 \text{ ksi}$$

Next, it is necessary to check whether the stress block depth is greater or less than the average flange thickness of 4.5 in. On the assumption that it is not greater than the flange thickness, Eq. (19.10) is used:

$$a = \frac{0.765 \times 248}{0.85 \times 4 \times 12} = 4.65 \text{ in.}$$

It is concluded from this trial calculation that a actually exceeds h_f, so the trial calculation is not valid and equations for flanged members must be used. The steel that acts with the overhanging flanges is found from Eq. (19.12) to be

$$A_{pf} = \frac{0.85 \times 4 \cdot 12 - 4 \cdot 4.5}{248} = 0.494 \text{ in}^2$$

and from Eq. (19.13),

$$A_{pw} = 0.765 - 0.494 = 0.271 \text{ in}^2$$

The actual stress block depth is now found from Eq. (19.15):

$$a = \frac{0.271 \times 248}{0.85 \times 4 \times 4} = 4.94 \text{ in.}$$

$$c = \frac{a}{\beta_1} = \frac{4.94}{0.85} = 5.81$$

A check should now be made to determine if the beam can be considered underreinforced. From Eq. (19.16),

$$\frac{c}{d_t} = \frac{5.81}{17.19} = 0.338$$

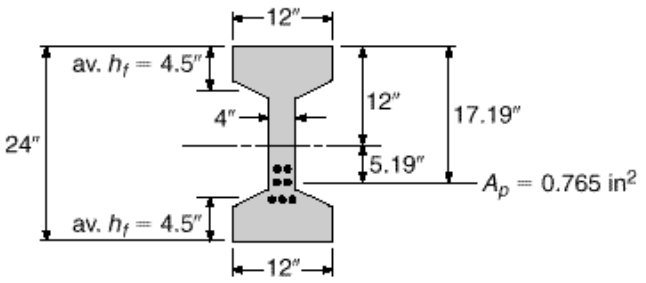

FIGURE 19.13
Post-tensioned beam of Example 19.2.

This is less than 0.375 for $\cdot_t \geq 0.005$, confirming that this can be considered to be an underreinforced prestressed beam and $\cdot = 0.90$. The nominal flexural strength, from Eq. (19.14*b*), is

$$M_n = 0.271 \times 248 \cdot 17.19 - 2.47 \cdot + 0.85 \times 4 \cdot 12 - 4 \cdot 4.5 \cdot 17.19 - 2.25 \cdot$$
$$= 2818 \text{ in-kips} = 235 \text{ ft-kips}$$

and, finally, the design strength is $\cdot M_n = 211$ ft-kips.

19.8 Partial Prestressing

Early in the development of prestressed concrete, the goal of prestressing was the complete elimination of concrete tensile stress at service load. This kind of design, in which the service load tensile stress limit $f_{ts} = 0$, is often referred to as *full prestressing*.

While full prestressing offers many advantages over nonprestressed construction, some problems can arise. Heavily prestressed beams, particularly those for which full live load is seldom in place, may have excessively large upward deflection, or camber, which will increase with time because of concrete creep under the eccentric prestress force. Fully prestressed beams may also have a tendency for severe longitudinal shortening, causing large restraint forces unless special provision is made to permit free movement at one end of each span. If shortening is permitted to occur freely, prestress losses due to elastic and creep deformation may be large. Furthermore, if heavily prestressed beams are overloaded to failure, they may fail in a sudden and brittle mode, with little warning before collapse.

Today there is general recognition of the advantages of *partial prestressing*, in which flexural tensile stress and some limited cracking is permitted under full service load. That full load may be infrequently applied. Typically, many beams carry only dead load much of the time, or dead load plus only part of the service live load. Under these conditions, a partially prestressed beam would normally not be subject to flexural tension, and cracks that form occasionally, when the full live load is in place, would close completely when that live load is removed. Controlled cracks prove no more objectionable in prestressed concrete structures than in reinforced concrete structures. With partial prestressing, excessive camber and troublesome axial shortening are avoided. Should overloading occur, there will be ample warning of distress, with extensive cracking and large deflections (Refs. 19.10 to 19.13).

Although the amount of prestressing steel may be reduced in partially prestressed beams compared with fully prestressed beams, a proper safety margin must still be maintained, and to achieve the necessary flexural strength, partially prestressed beams may require additional tensile reinforcement. In fact, partially prestressed beams are often defined as beams in which (a) flexural cracking is permitted at full service load and (b) the main flexural tension reinforcement includes both prestressed and nonprestressed steel. Analysis indicates, and tests confirm, that such nonprestressed steel is fully stressed to f_y at flexural failure.

The ACI Code does not specifically mention partial prestressing but does include the concept explicitly in the classification of flexural members. Class T flexural members require service level stress checks and have maximum allowable tensile stresses above the modulus of rupture. Class C flexural members do not require stress checks at service load but do require crack control checks (Section 19.18). The designations

of Class T and Class C flexural members brings the ACI Code into closer agreement with European practice (Refs. 19.13 to 19.15).

The three classes of prestressed flexural members, U, T, and C, provide the designer with considerable flexibility in achieving economical designs. To attain the required strength, supplemental reinforcement in the form of nonprestressed ordinary steel or unstressed prestressing strand may be required. Reinforcing bars are less expensive than high-strength prestressing steel. Strand, however, at twice the cost of ordinary reinforcement, provides 3 times the strength. Labor costs for bar placement are generally similar to those for placing unstressed strand on site. Similarly, the addition of a small number of strands in a plant prestressing bed is often more economical than adding reinforcing bars. The designer may select the service level performance strategy best suited for the project. A criterion that includes no tensile stress under dead load and a tensile stress less than the modulus of rupture at the service live load is possible with Class U and T flexural members, while Class C members use prestressing primarily for deflection control.

The choice of a suitable degree of prestress is governed by a number of factors. These include the nature of the loading (for example, highway or railroad bridges, and storage warehouses), the ratio of live to dead load, the frequency of occurrence of the full service load, and the presence of a corrosive environment.

19.9 Flexural Design Based on Concrete Stress Limits

As in reinforced concrete, problems in prestressed concrete can be separated generally as analysis problems or design problems. For the former, with the applied loads, the concrete cross section, steel area, and the amount and point of application of the prestress force known, Eqs. (19.1) to (19.4) permit the direct calculation of the resulting concrete stresses. The equations in Section 19.7 will predict the flexural strength. However, if the dimensions of a concrete section, the steel area and centroid location, and the amount of prestress are to be found—given the loads, limiting stresses, and required strength—the problem is complicated by the many interrelated variables.

There are at least three practical approaches to the flexural design of a prestressed concrete member. Some engineers prefer to assume a concrete section, calculate the required prestress force and eccentricities for what will probably be the controlling load stage, then check the stresses at all stages using the preceding equations, and finally check the flexural strength. The trial section is then revised if necessary. If a beam is to be chosen from a limited number of standard shapes, as is often the case for shorter spans and ordinary loads, this procedure is probably best. For longer spans or when customized shapes are used, a more efficient member may result by designing the cross section so that the specified concrete stress limits of Table 19.2 are closely matched. This cross section, close to "ideal" from the limit stress viewpoint, may then be modified to meet functional requirements (e.g., providing a broad top flange for a bridge deck) or to meet strength requirements, if necessary. Equations facilitating this approach will be developed in this section. A third method of design is based on load balancing, using the concept of equivalent loads (see Section 19.2b). A trial section is chosen, after which the prestress force and tendon profile are selected to provide uplift forces as to just balance a specified load. Modifications may then be made, if needed, to satisfy stress limits or strength requirements. This third approach will be developed in Section 19.12.

Notation is established pertaining to the allowable concrete stresses at limiting stages as follows:

f_{ci} = allowable compressive stress immediately after transfer

f_{ti} = allowable tensile stress immediately after transfer

f_{cs} = allowable compressive stress at service load, after all losses

f_{ts} = allowable tensile stress at service load, after all losses

The values of these limit stresses are normally set by specification (see Table 19.2).

a. Beams with Variable Eccentricity

For a typical Class U or T beam in which the tendon eccentricity is permitted to vary along the span, flexural stress distributions in the concrete at the maximum moment section are shown in Fig. 19.14*a*. The eccentric prestress force, having an initial value of P_i, produces the linear stress distribution (1). Because of the upward camber of the

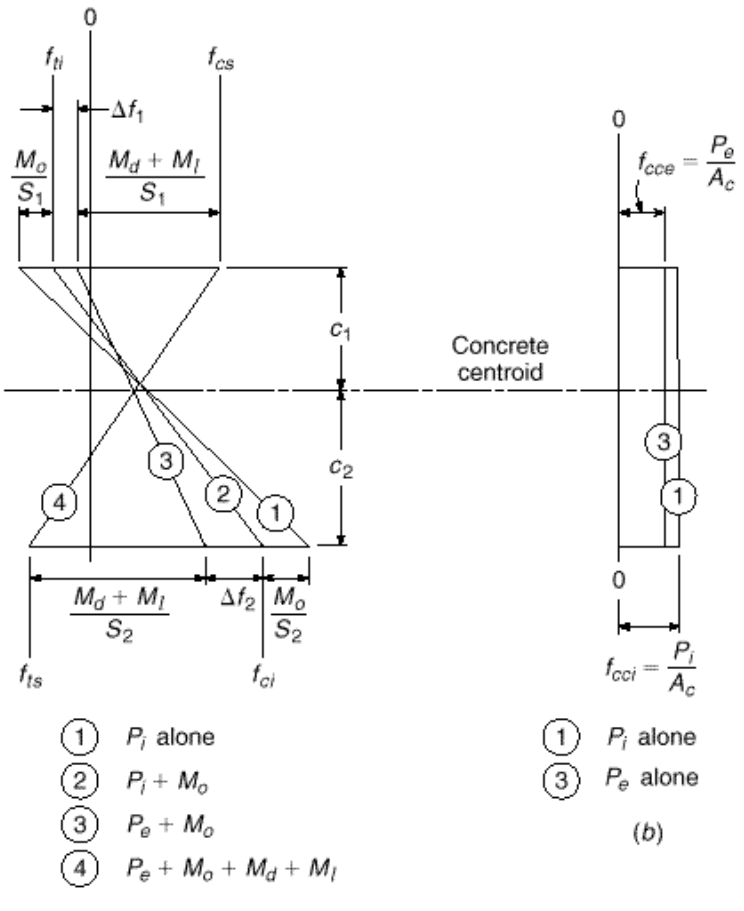

FIGURE 19.14
Flexural stress distributions for beams with variable eccentricity: (*a*) maximum moment section; (*b*) support section.

beam as that force is applied, the self-weight of the member is immediately introduced, the flexural stresses resulting from the moment M_o are superimposed, and the distribution (2) is the first that is actually attained. At this stage, the tension at the top surface is not to exceed f_{ti} and the compression at the bottom surface is not to exceed f_{ci}, as suggested by Fig. 19.14*a*.

It will be assumed that all the losses occur at this stage, and that the stress distribution gradually changes to distribution (3). The losses produce a reduction of tension in the amount Δf_1 at the top surface, and a reduction of compression in the amount Δf_2 at the bottom surface.

As the superimposed dead load moment M_d and the service live load moment M_l are introduced, the associated flexural stresses, when superimposed on stresses already present, produce distribution (4). At this stage, the tension at the bottom surface must not be greater than f_{ts}, and the compression at the top of the section must not exceed f_{cs} as shown.

The requirements for the sections moduli S_1 and S_2 with respect to the top and bottom surfaces, respectively, are

$$S_1 \geq \frac{M_d + M_l}{f_{1r}} \tag{a}$$

$$S_2 \geq \frac{M_d + M_l}{f_{2r}} \tag{b}$$

where the available stress ranges f_{1r} and f_{2r} at the top and bottom face can be calculated from the specified stress limits f_{ti}, f_{cs}, f_{ts}, and f_{ci}, once the stress changes Δf_1 and Δf_2, associated with prestress loss, are known.

The effectiveness ratio R is defined as

$$R = \frac{P_e}{P_i} \tag{19.18}$$

Thus, the loss in prestress force is

$$P_i - P_e = \cdot 1 - R \cdot P_i \tag{19.19}$$

The changes in stress at the top and bottom faces, Δf_1 and Δf_2, as losses occur, are equal to $(1 - R)$ times the corresponding stresses due to the initial prestress force P_i *acting alone*:

$$\cdot f_1 = \cdot 1 - R \cdot \cdot f_{ti} + \frac{M_o}{S_1} \cdot \tag{c}$$

$$\cdot f_2 = \cdot 1 - R \cdot \cdot -f_{ci} + \frac{M_o}{S_2} \cdot \tag{d}$$

where Δf_1 is a reduction of tension at the top surface and Δf_2 is a reduction of compression at the bottom surface.† Thus, the stress ranges available as the superimposed load moments $M_d + M_l$ are applied are

$$\begin{aligned} f_{1r} &= f_{ti} - \cdot f_1 - f_{cs} \\ &= Rf_{ti} - \cdot 1 - R \cdot \frac{M_o}{S_1} - f_{cs} \end{aligned} \tag{e}$$

† Note that the stress limits such as f_{ti} and other specific points along the stress axis are considered signed quantities, whereas stress changes such as $M_o \cdot S_1$ and Δf_2 are taken as absolute values.

and

$$f_{2r} = f_{ts} - f_{ci} - \cdot f_2$$

$$= f_{ts} - Rf_{ci} - \cdot 1 - R \cdot \frac{M_o}{S_2} \qquad (f)$$

The minimum acceptable value of S_1 is thus established:

$$S_1 \geq \frac{M_d + M_l}{Rf_{ti} - \cdot 1 - R \cdot \frac{M_o}{S_1} - f_{cs}}$$

or

$$S_1 \geq \frac{\cdot 1 - R \cdot M_o + M_d + M_l}{Rf_{ti} - f_{cs}} \qquad (19.20)$$

Similarly, the minimum value of S_2 is

$$S_2 \geq \frac{\cdot 1 - R \cdot M_o + M_d + M_l}{f_{ts} - Rf_{ci}} \qquad (19.21)$$

The cross section must be selected to provide at least these values of S_1 and S_2. Furthermore, since $I_c = S_1 c_1 = S_2 c_2$, the centroidal axis must be located such that

$$\frac{c_1}{c_2} = \frac{S_2}{S_1} \qquad (g)$$

or in terms of the total section depth $h = c_1 + c_2$

$$\frac{c_1}{h} = \frac{S_2}{S_1 + S_2} \qquad (19.22)$$

From Fig. 19.14*a*, the concrete centroidal stress under initial conditions f_{cci} is given by

$$f_{cci} = f_{ti} - \frac{c_1}{h} \cdot f_{ti} - f_{ci} \cdot \qquad (19.23)$$

The initial prestress force is easily obtained by multiplying the value of the concrete centroidal stress by the concrete cross-sectional area A_c.

$$P_i = A_c f_{cci} \qquad (19.24)$$

The eccentricity of the prestress force may be found by considering the flexural stresses that must be imparted by the bending moment $P_i e$. With reference to Fig. 19.14, the flexural stress at the top surface of the beam resulting from the eccentric prestress force alone is

$$\frac{P_i e}{S_1} = \cdot f_{ti} - f_{cci} \cdot + \frac{M_o}{S_1} \qquad (h)$$

from which the required eccentricity is

$$e = \cdot f_{ti} - f_{cci} \cdot \frac{S_1}{P_i} + \frac{M_o}{P_i} \qquad (19.25)$$

Summarizing the design process to determine the best cross section and the required prestress force and eccentricity based on stress limitations: the required section

moduli with respect to the top and bottom surfaces of the member are found from Eqs. (19.20) and (19.21) with the centroidal axis located using Eq. (19.22). Concrete dimensions are chosen to satisfy these requirements as nearly as possible. The concrete centroidal stress for this ideal section is given by Eq. (19.23), the desired initial prestress force by Eq. (19.24), and its eccentricity by Eq. (19.25).

In practical situations, very seldom will the concrete section chosen have exactly the required values of S_1 and S_2 as found by this method, nor will the concrete centroid be exactly at the theoretically ideal level. Rounding concrete dimensions upward, providing broad flanges for functional reasons, or using standardized cross-sectional shapes will result in a member whose section properties will exceed the minimum requirements. In such a case, the stresses in the concrete as the member passes from the unloaded stage to the full service load stage will stay within the allowable limits, but the limit stresses will not be obtained exactly. An infinite number of combinations of prestress force and eccentricity will satisfy the requirements. Usually, the design requiring the lowest value of prestress force, and the largest practical eccentricity, will be the most economical.

The total eccentricity in Eq. (19.25) includes the term M_o / P_i. As long as the beam is deep enough to allow this full eccentricity, the girder dead load moment is carried with no additional penalty in terms of prestress force, section, or stress range. This ability to carry the beam dead load "free" is a major contribution of variable eccentricity.

The stress distributions shown in Fig. 19.14*a*, on which the design equations are based, apply at the maximum moment section of the member. Elsewhere, M_o is less and, consequently, the prestress eccentricity or the force must be reduced if the stress limits f_{ti} and f_{ci} are not to be exceeded. In many cases, tendon eccentricity is reduced to zero at the support sections, where all moments due to transverse load are zero. In this case, the stress distributions of Fig. 19.14*b* are obtained. The stress in the concrete is uniformly equal to the centroidal value f_{cci} under conditions of initial prestress and f_{cce} after losses.

EXAMPLE 19.3

Design of beam with variable eccentricity tendons. A post-tensioned prestressed concrete beam is to carry an intermittent live load of 1000 lb/ft and superimposed dead load of 500 lb/ft, in addition to its own weight, on a 40 ft simple span. Normal-density concrete will be used with design strength $f'_c = 6000$ psi. It is estimated that, at the time of transfer, the concrete will have attained 70 percent of f'_c, or 4200 psi. Time-dependent losses may be assumed to be 15 percent of the initial prestress, giving an effectiveness ratio of 0.85. Determine the required concrete dimensions, magnitude of prestress force, and eccentricity of the steel centroid based on ACI stress limitations for a Class U beam, as given in Sections 19.4 and 19.5.

SOLUTION. Referring to Table 19.2, the stress limits are:

$$f_{ci} = -0.60 \times 4200 = 2520 \text{ psi}$$

$$f_{ti} = 3\sqrt{4200} = +195 \text{ psi}$$

$$f_{cs} = -0.60 \times 6000 = -3600 \text{ psi}$$

$$f_{ts} = 7.5\sqrt{6000} = +581 \text{ psi}$$

The self-weight of the girder will be estimated at 250 lb/ft. The service moments due to transverse loading are

$$M_o = \frac{1}{8} \times 0.250 \times 40^2 = 50 \text{ ft-kips}$$

$$M_d + M_l = \frac{1}{8} \times 1.500 \times 40^2 = 300 \text{ ft-kips}$$

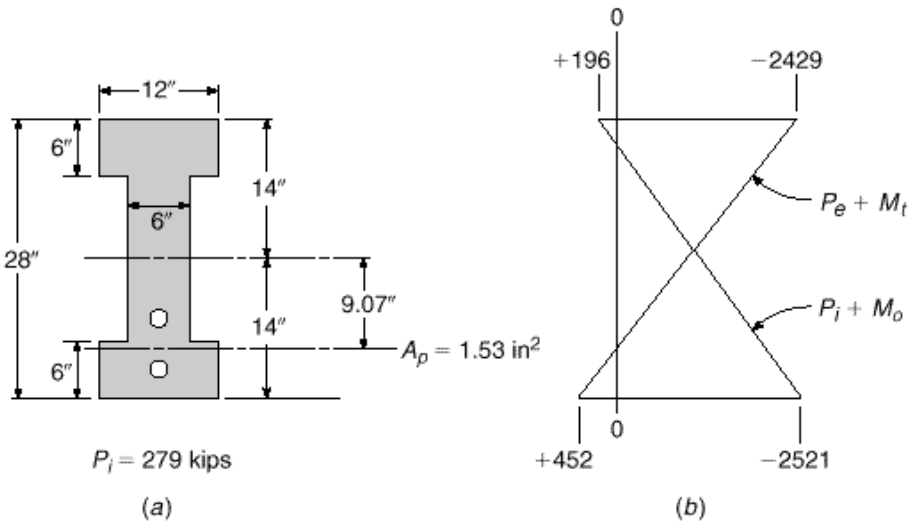

FIGURE 19.15
Design example of beam with variable eccentricity of tendons: (*a*) cross section dimensions; (*b*) concrete stresses at midspan (psi).

The required section moduli with respect to the top and bottom surfaces of the concrete beam are found from Eqs. (19.20) and (19.21).

$$S_1 \geq \frac{(1 - R)M_o + M_d + M_l}{Rf_{ti} - f_{cs}} = \frac{(0.15 \times 50 + 300)12{,}000}{0.85 \times 195 + 3600} = 980 \text{ in}^3$$

$$S_2 \geq \frac{(1 - R)M_o + M_d + M_l}{f_{ts} - Rf_{ci}} = \frac{(0.15 \times 50 + 300)12{,}000}{581 + 0.85 \times 2520} = 1355 \text{ in}^3$$

The values obtained for S_1 and S_2 suggest that an asymmetrical section is most appropriate. However, a symmetrical section is selected for simplicity and to ensure sufficient compression area for flexural strength. The 28-in. deep I section shown in Fig. 19.15*a* will meet the requirements and has the following properties:

$$I_c = 19{,}904 \text{ in}^4$$
$$S = 1422 \text{ in}^3$$
$$A_c = 240 \text{ in}^2$$
$$r^2 = 82.9 \text{ in}^2$$
$$w_o = 250 \text{ lb/ft} \quad \text{(as assumed)}$$

Next, the concrete centroidal stress is found from Eq. (19.23):

$$f_{cci} = f_{ti} - \frac{c_1}{h}(f_{ti} - f_{ci}) = 195 - \frac{1}{2}(195 + 2520) = -1163 \text{ psi}$$

and from Eq. (19.24) the initial prestress force is

$$P_i = A_c f_{cci} = 240 \times 1.163 = 279 \text{ kips}$$

From Eq. (19.25), the required tendon eccentricity at the maximum moment section of the beam is

$$e = (f_{ti} - f_{cci})\frac{S_1}{P_i} + \frac{M_o}{P_i} = (195 + 1163)\frac{1422}{279{,}000} + \frac{50 \times 12{,}000}{279{,}000}$$

$$= 9.07 \text{ in.}$$

Elsewhere along the span, the eccentricity will be reduced so that the concrete stress limits will not be violated.

The required initial prestress force of 279 kips will be provided using tendons consisting of $\frac{1}{2}$ in. diameter Grade 270 low-relaxation strands (see Section 2.16). The minimum tensile strength is $f_{pu} = 270$ ksi, and the yield strength may be taken as $f_{py} = 0.90 \times 270 = 243$ ksi. According to the ACI Code (see Section 19.4), the permissible stress in the strand immediately after transfer must not exceed $0.82 f_{py} = 199$ ksi or $0.74 f_{pu} = 200$ ksi. The first criterion controls. The required area of prestressing steel is

$$A_{ps} = \frac{279}{199} = 1.40 \text{ in}^2$$

The cross-sectional area of one $\frac{1}{2}$ in. diameter strand is 0.153 in^2; hence, the number of strands required is

$$\text{Number of strands} = \frac{1.40}{0.153} = 9.2$$

Two five-strand tendons will be used, as shown in Fig. 19.15*a*, each stressed to 139.5 kips immediately following transfer.

It is good practice to check the calculations by confirming that stress limits are not exceeded at critical load stages. The top and bottom surface concrete stresses produced, in this case, by the separate loadings are:

$$P_i\colon\ f_1 = -\frac{279{,}000}{240}\left(1 - \frac{9.07 \times 14}{82.9}\right) = +618 \text{ psi}$$

$$f_2 = -\frac{279{,}000}{240}\left(1 + \frac{9.07 \times 14}{82.9}\right) = -2943 \text{ psi}$$

$$P_e\colon\ f_1 = 0.85 \times 618 = 525 \text{ psi}$$

$$f_2 = 0.85\,(-2943) = -2502 \text{ psi}$$

$$M_o\colon\ f_1 = -\frac{50 \times 12{,}000}{1422} = -422 \text{ psi}$$

$$f_2 = +422 \text{ psi}$$

$$M_d + M_l\colon\ f_1 = -\frac{300 \times 12{,}000}{1422} = -2532 \text{ psi}$$

$$f_2 = +2532 \text{ psi}$$

Thus, when the initial prestress force of 279 kips is applied and the beam self-weight acts, the top and bottom stresses in the concrete at midspan are, respectively,

$$f_1 = +618 - 422 = +196 \text{ psi}$$

$$f_2 = -2943 + 422 = -2521 \text{ psi}$$

When the prestress force has decreased to its effective value of 237 kips and the full service load is applied, the concrete stresses are

$$f_1 = +525 - 422 - 2532 = -2429 \text{ psi}$$

$$f_2 = -2502 + 422 + 2532 = +452 \text{ psi}$$

These stress distributions are shown in Fig. 19.15*b*. Comparison with the specified limit stresses confirms that the design is satisfactory.

b. Beams with Constant Eccentricity

The design method presented in the previous section was based on stress conditions at the maximum moment section of a beam, with the maximum value of moment M_o resulting from the self-weight immediately being superimposed. If P_i and e were to be held constant along the span, as is often convenient in pretensioned prestressed construction, then the stress limits f_{ti} and f_{ci} would be exceeded elsewhere along the span, where M_o is less than its maximum value. To avoid this condition, the constant eccentricity must be less than that given by Eq. (19.25). Its maximum value is given by conditions at the support of a simple span, where M_o is zero.

Figure 19.16 shows the flexural stress distributions at the support and midspan sections for a beam with constant eccentricity. In this case, the stress limits f_{ti} and f_{ci} are not to be violated when the eccentric prestress moment acts alone, as at the supports. The stress changes Δf_1 and Δf_2 as losses occur are equal to $(1 - R)$ times the top and bottom surface stresses, respectively, due to initial prestress alone:

$$\Delta f_1 = (1 - R) f_{ti} \qquad (a)$$

$$\Delta f_2 = (1 - R)(-f_{ci}) \qquad (b)$$

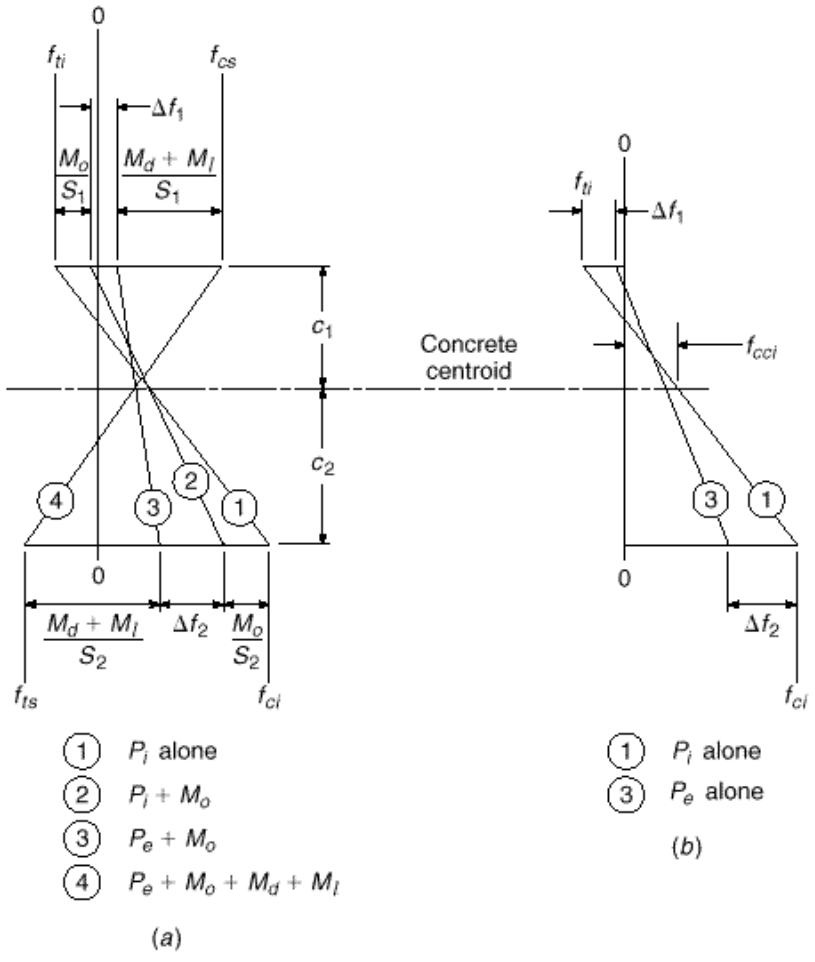

FIGURE 19.16
Flexural stress distributions for beam with constant eccentricity of tendons: (*a*) maximum moment section; (*b*) support section.

In this case, the available stress ranges between limit stresses must provide for the effect of M_o as well as M_d and M_l, as seen from Fig. 19.16*a*, and are

$$f_{1r} = f_{ti} - \cdot f_1 - f_{cs}$$
$$= Rf_{ti} - f_{cs} \qquad (c)$$
$$f_{2r} = f_{ts} - f_{ci} - \cdot f_2$$
$$= f_{ts} - Rf_{ci} \qquad (d)$$

and the requirements on the section moduli are that

$$S_1 \geq \frac{M_o + M_d + M_l}{Rf_{ti} - f_{cs}} \qquad (19.26)$$

$$S_2 \geq \frac{M_o + M_d + M_l}{f_{ts} - Rf_{ci}} \qquad (19.27)$$

The concrete centroidal stress may be found by Eq. (19.23) and the initial prestress force by Eq. (19.24) as before. However, the expression for required eccentricity differs. In this case, referring to Fig. 19.16*b*,

$$\frac{P_i e}{S_1} = f_{ti} - f_{cci} \qquad (e)$$

from which the required eccentricity is

$$e = \cdot f_{ti} - f_{cci} \cdot \frac{S_1}{P_i} \qquad (19.28)$$

A significant difference between beams with variable eccentricity and those with constant eccentricity will be noted by comparing Eqs. (19.20) and (19.21) with the corresponding Eqs. (19.26) and (19.27). In the first case, the section modulus requirement is governed mainly by the superimposed load moments M_d and M_l. Almost all of the self-weight is carried "free," that is, without increasing section modulus or prestress force, by the simple expedient of increasing the eccentricity along the span by the amount $M_o \cdot P_i$. In the second case, the eccentricity is controlled by conditions at the supports, where M_o is zero, and the full moment M_o due to self-weight must be included in determining section moduli. Nevertheless, beams with constant eccentricity are often used for practical reasons.

EXAMPLE 19.4

Design of beam with constant eccentricity tendons. The beam in the preceding example is to be redesigned using straight tendons with constant eccentricity. All other design criteria are the same as before. At the supports, a temporary concrete tensile stress $f_{ti} = 6 \cdot \sqrt{f'_{ci}} = 390$ psi is permitted.

SOLUTION. Anticipating a somewhat less efficient beam, the dead load estimate will be increased to 270 lb/ft in this case. The resulting moment M_o is 54 ft-kips. The moment due to superimposed dead load and live load is 300 ft-kips as before.

Using Eqs. (19.26) and (19.27), the requirements for section moduli are

$$S_1 \geq \frac{M_o + M_d + M_l}{Rf_{ti} - f_{cs}} = \frac{54 + 300 \cdot 12{,}000}{0.85 \times 390 + 3600} = 1080 \text{ in}^3$$

$$S_2 \geq \frac{M_o + M_d + M_l}{f_{ts} - Rf_{ci}} = \frac{54 + 300 \cdot 12{,}000}{581 + 0.85 \times 2520} = 1560 \text{ in}^3$$

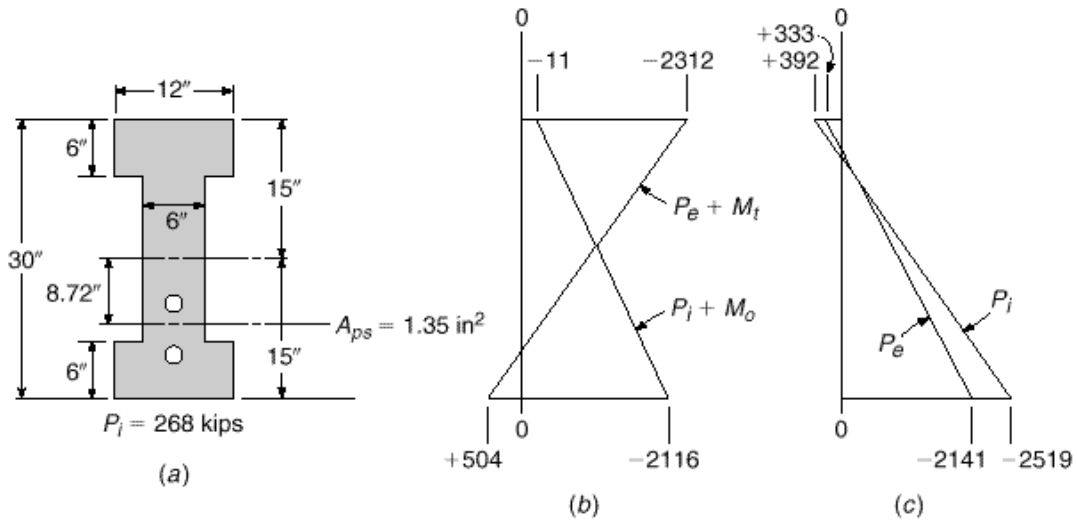

FIGURE 19.17
Design example of beam with constant eccentricity of tendons: (*a*) cross section dimensions; (*b*) stresses at midspan (psi); (*c*) stresses at supports (psi).

Once again, a symmetrical section will be chosen. Flange dimensions and web width will be kept unchanged compared with the previous example, but in this case a beam depth of 30.0 in. is required. The dimensions of the cross section are shown in Fig. 19.17*a*. The following properties are obtained:

$$I_c = 24{,}084 \text{ in}^4$$
$$S = 1606 \text{ in}^3$$
$$A_c = 252 \text{ in}^2$$
$$r^2 = 95.6 \text{ in}^2$$
$$w_o = 263 \text{ lb/ft} \quad \text{close to the assumed value}$$

The concrete centroidal stress, from Eq. (19.23), is

$$f_{cci} = f_{ti} - \frac{c_1}{h}(f_{ti} - f_{ci}) = 390 - \frac{1}{2}(390 + 2520) = -1065 \text{ psi}$$

and from Eq. (19.24), the initial prestress force is

$$P_i = A_c f_{cci} = 252 \times 1.065 = 268 \text{ kips}$$

From Eq. (19.28), the required constant eccentricity is

$$e = (f_{ti} - f_{cci})\frac{S_1}{P_i} = (390 + 1065)\frac{1606}{268{,}000} = 8.72 \text{ in.}$$

Again, two tendons will be used to provide the required prestress force, each composed of multiple $\frac{1}{2}$ in. diameter Grade 270 low-relaxation strands. With the maximum permissible stress in the stranded cable just after transfer of 199 ksi, the total required steel area is

$$A_{ps} = \frac{268}{199} = 1.35 \text{ in}^2$$

A total of nine strands is required. For practical reasons, two identical five-strand tendons will be used as before, in this case being stressed to 134 kips.

The calculations will be checked by verifying the concrete stresses at the top and bottom of the beam for the critical load stages. The component stress contributions are

$$P_i\text{: } f_1 = -\frac{268{,}000}{252}\left(1 - \frac{8.72 \times 15.0}{95.6}\right) = +392 \text{ psi}$$

$$f_2 = -\frac{268{,}000}{252}\left(1 + \frac{8.72 \times 15.0}{95.6}\right) = -2519 \text{ psi}$$

$$P_e\text{: } f_1 = 0.85 \times 392 = +333 \text{ psi}$$

$$f_2 = 0.85(-2519) = -2141 \text{ psi}$$

$$M_o\text{: } f_1 = -\frac{54 \times 12{,}000}{1606} = -403 \text{ psi}$$

$$f_2 = +403 \text{ psi}$$

$$M_d + M_l\text{: } f_1 = -\frac{300 \times 12{,}000}{1606} = -2242 \text{ psi}$$

$$f_2 = +2242 \text{ psi}$$

Superimposing the appropriate stress contributions, the stress distributions in the concrete at midspan and at the supports are obtained, as shown in Fig. 19.17*b* and *c*, respectively. When the initial prestress force of 268 kips acts alone, as at the supports, the stresses at the top and bottom surfaces are

$$f_1 = +392 \text{ psi}$$

$$f_2 = -2519 \text{ psi}$$

After losses, the prestress force is reduced to 228 kips and the support stresses are reduced accordingly. At midspan, the beam weight is immediately superimposed, and stresses resulting from P_i plus M_o are

$$f_1 = +392 - 403 = -11 \text{ psi}$$

$$f_2 = -2519 + 403 = -2116 \text{ psi}$$

When the full service load acts, together with P_e, the midspan stresses are

$$f_1 = +333 - 403 - 2242 = -2312 \text{ psi}$$

$$f_2 = -2141 + 403 + 2242 = +504 \text{ psi}$$

If we check against the specified limiting stresses, it is evident that the design is satisfactory in this respect at the critical load stages and locations.

19.10 SHAPE SELECTION

One of the special features of prestressed concrete design is the freedom to select cross-section proportions and dimensions to suit the special requirements of the job at hand. The member depth can be changed, the web thickness modified, and the flange widths and thicknesses varied independently to produce a beam with nearly ideal proportions for a given case.

Several common precast shapes are shown in Fig. 19.18. Some of these are standardized and mass produced, employing reusable steel or fiberglass forms. Others are individually proportioned for large and important works. The double T (Fig. 19.18*a*) is probably the most widely used cross section in U.S. prestressed construction. A flat

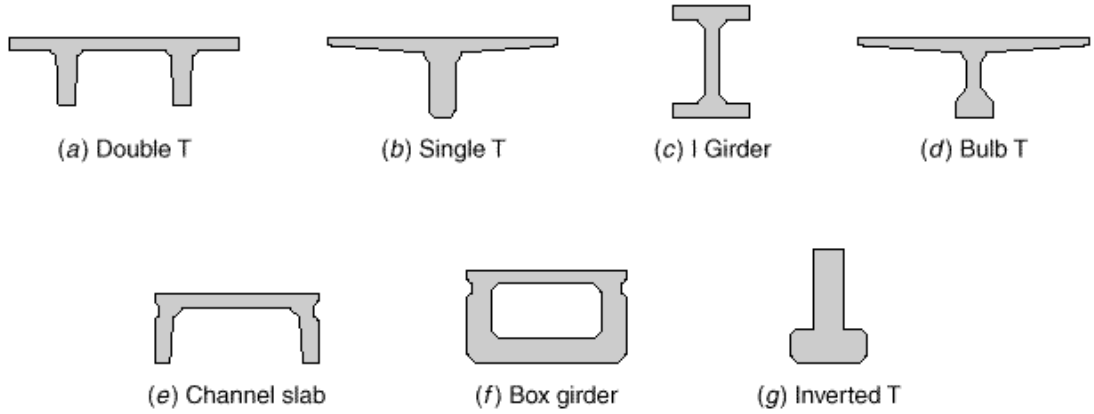

FIGURE 19.18
Typical beam cross sections.

surface is provided, 4 to 12 ft wide. Slab thicknesses and web depths vary, depending upon requirements. Spans to 60 ft are not unusual. The single T (Fig. 19.18*b*) is more appropriate for longer spans, to 120 ft, and heavier loads. The I and bulb T sections (Fig. 19.18*c* and *d*) are widely used for bridge spans and roof girders up to about 140 ft, while the channel slab (Fig. 19.18*e*) is suitable for floors in the intermediate span range. The box girder (Fig. 19.18*f*) is advantageous for bridges of intermediate and major span. The inverted T section (Fig. 19.18*g*) provides a bearing ledge to carry the ends of precast deck members spanning in the perpendicular direction. Local precasting plants can provide catalogs of available shapes. This information is also available in the *PCI Design Handbook* (Ref. 19.8).

As indicated, the cross section may be symmetrical or unsymmetrical. An unsymmetrical section is a good choice (1) if the available stress ranges f_{1r} and f_{2r} at the top and bottom surfaces are not the same; (2) if the beam must provide a flat, useful surface as well as offering load-carrying capacity; (3) if the beam is to become a part of composite construction, with a cast-in-place slab acting together with a precast web; or (4) if the beam must provide support surfaces, such as shown in Fig. 19.18*g*. In addition, T sections provide increased flexural strength, since the internal arm of the resisting couple at maximum design load is greater than for rectangular sections.

Generally speaking, I, T, and box sections with relatively thin webs and flanges are more efficient than members with thicker parts. However, several factors limit the gain in efficiency that may be obtained in this way. These include the instability of very thin overhanging compression parts, the vulnerability of thin parts to breakage in handling (in the case of precast construction), and the practical difficulty of placing concrete in very thin elements. The designer must also recognize the need to provide adequate spacing and concrete protection for tendons and anchorages, the importance of construction depth limitations, and the need for lateral stability if the beam is not braced by other members against buckling (Ref. 19.16).

19.11 TENDON PROFILES

The equations developed in Section 19.9a for members with variable tendon eccentricity establish the requirements for section modulus, prestress force, and eccentricity at the maximum moment section of the member. Elsewhere along the span, the

eccentricity of the steel must be reduced if the concrete stress limits for the unloaded stage are not to be exceeded. (Alternatively, the section must be increased, as demonstrated in Section 19.9b.) Conversely, there is a minimum eccentricity, or upper limit for the steel centroid, such that the limiting concrete stresses are not exceeded when the beam is in the full service load stage.

Limiting locations for the prestressing steel centroid at any point along the span can be established using Eqs. (19.2) and (19.4), which give the values of concrete stress at the top and bottom of the beam in the unloaded and service load stages, respectively. The stresses produced for those load stages should be compared with the limiting stresses applicable in a particular case, such as the ACI stress limits of Table 19.2. This permits a solution for tendon eccentricity e as a function of distance x along the span.

To indicate that both eccentricity e and moments M_o or M_t are functions of distance x from the support, they will be written as $e(x)$ and $M_o(x)$ or $M_t(x)$, respectively. In writing statements of inequality, it is convenient to designate tensile stress as larger than zero and compressive stress as smaller than zero. Thus, $+450 > -1350$, and $-600 > -1140$, for example.

Considering first the unloaded stage, the tensile stress at the top of the beam must not exceed f_{ti}. From Eq. (19.2a),

$$f_{ti} \geq -\frac{P_i}{A_c}\cdot\left(1-\frac{e\cdot x\cdot c_1}{r^2}\right)-\frac{M_o\cdot x}{S_1} \qquad (a)$$

Solving for the maximum eccentricity gives

$$e\cdot x \leq \frac{f_{ti}S_1}{P_i}+\frac{S_1}{A_c}+\frac{M_o\cdot x}{P_i} \qquad (19.29)$$

At the bottom of the unloaded beam, the stress must not exceed the limiting initial compression. From Eq. (19.2b),

$$f_{ci} \leq -\frac{P_i}{A_c}\cdot\left(1+\frac{e\cdot x\cdot c_2}{r^2}\right)+\frac{M_o\cdot x}{S_2} \qquad (b)$$

Hence, the second lower limit for the steel centroid is

$$e\cdot x \leq -\frac{f_{ci}S_2}{P_i}-\frac{S_2}{A_c}+\frac{M_o\cdot x}{P_i} \qquad (19.30)$$

Now considering the member in the fully loaded stage, the upper limit values for the eccentricity may be found. From Eq. (19.4a),

$$f_{cs} \leq -\frac{P_e}{A_c}\cdot\left(1-\frac{e\cdot x\cdot c_1}{r^2}\right)-\frac{M_t\cdot x}{S_1} \qquad (c)$$

from which

$$e\cdot x \geq \frac{f_{cs}S_1}{P_e}+\frac{S_1}{A_c}+\frac{M_t\cdot x}{P_e} \qquad (19.31)$$

and using Eq. (19.4b)

$$f_{ts} \geq -\frac{P_e}{A_c}\cdot\left(1+\frac{e\cdot x\cdot c_2}{r^2}\right)+\frac{M_t\cdot x}{S_2} \qquad (d)$$

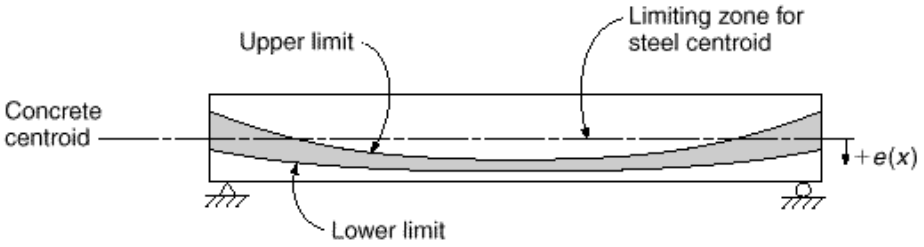

FIGURE 19.19
Typical limiting zone for centroid of prestressing steel.

from which

$$e \cdot x \cdot \geq -\frac{f_{ts} S_2}{P_e} - \frac{S_2}{A_c} + \frac{M_t \cdot x \cdot}{P_e} \tag{19.32}$$

Using Eqs. (19.29) and (19.30), the lower limit of tendon eccentricity is established at successive points along the span. Then, using Eqs. (19.31) and (19.32), the corresponding upper limit is established. This upper limit may well be negative, indicating that the tendon centroid may be above the concrete centroid at that location.

It is often convenient to plot the envelope of acceptable tendon profiles, as done in Fig. 19.19, for a typical case in which both dead and live loads are uniformly distributed. Any tendon centroid falling completely within the shaded zone would be satisfactory from the point of view of concrete stress limits. It should be emphasized that it is only the tendon centroid that must be within the shaded zone; individual cables are often outside of it.

The tendon profile actually used is often a parabolic curve or a catenary in the case of post-tensioned beams. The duct containing the prestressing steel is draped to the desired shape and held in that position by wiring it to the transverse web reinforcement, after which the concrete may be placed. In pretensioned beams, *deflected tendons* are often used. The cables are held down at midspan, at the third points, or at the quarter points of the span and held up at the ends, so that a smooth curve is approximated to a greater or lesser degree.

In practical cases, it is often not necessary to make a centroid zone diagram, such as is shown in Fig. 19.19. By placing the centroid at its known location at midspan, at or close to the concrete centroid at the supports, and with a near-parabolic shape between those control points, satisfaction of the limiting stress requirements is ensured. With nonprismatic beams, beams in which a curved concrete centroidal axis is employed, or with continuous beams, diagrams such as Fig. 19.19 are a great aid.

19.12 Flexural Design Based on Load Balancing

It was pointed out in Section 19.2b that the effect of a change in the alignment of a prestressing tendon in a beam is to produce a vertical force on the beam at that location. Prestressing a member with curved or deflected tendons, thus, has the effect of introducing a set of equivalent loads, and these may be treated just as any other loads in finding moments or deflections. Each particular tendon profile produces its own unique set of equivalent forces. Typical tendon profiles, with corresponding equivalent loads and moment diagrams, were illustrated in Fig. 19.2. Both Fig. 19.2 and Section 19.2b should be reviewed carefully.

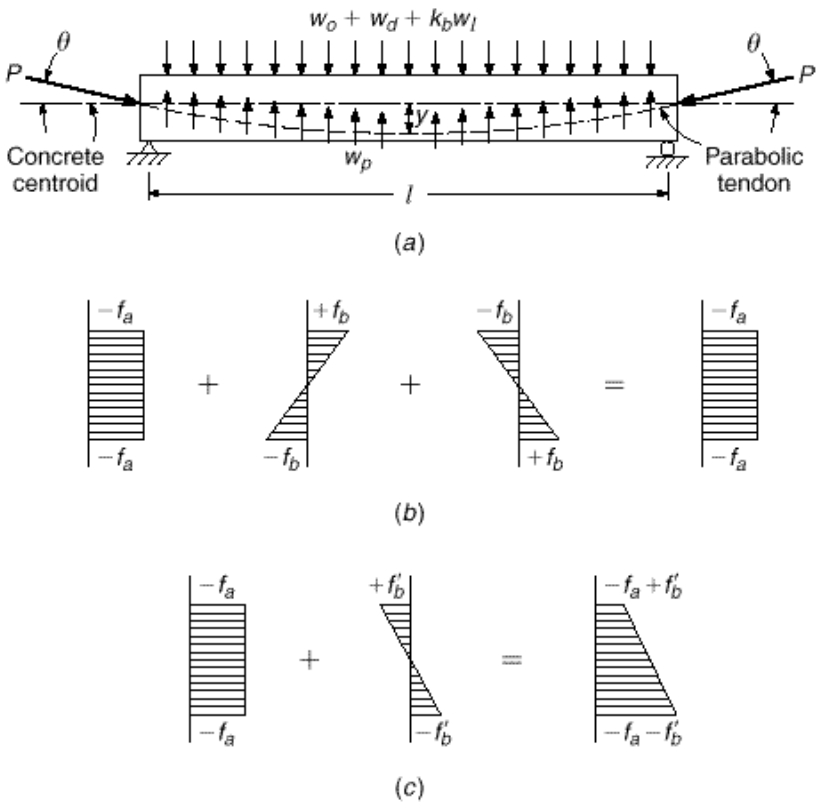

FIGURE 19.20
Load balancing for uniformly loaded beam: (*a*) external and equivalent loads; (*b*) concrete stresses resulting from axial and bending effects of prestress plus bending resulting from balanced external load; (*c*) concrete stresses resulting when load $k_b w_l$ is removed.

The equivalent load concept offers an alternative approach to the determination of required prestress force and eccentricity. The prestress force and tendon profile can be established so that external loads that will act are exactly counteracted by the vertical forces resulting from prestressing. The net result, for that particular set of external loads, is that the beam is subjected only to axial compression and no bending moment. The selection of the load to be balanced is left to the judgment of the designer. Often the balanced load chosen is the sum of the self-weight and superimposed dead load.

The design approach described in this section was introduced in the United States by T. Y. Lin in 1963 and is known as the *load-balancing method*. The fundamentals will be illustrated in the context of the simply supported, uniformly loaded beam shown in Fig. 19.20*a*. The beam is to be designed for a balanced load consisting of its own weight w_o, the superimposed dead load w_d, and some fractional part of the live load, denoted by $k_b w_l$. Since the external load is uniformly distributed, it is reasonable to adopt a tendon having a parabolic shape. It is easily shown that a parabolic tendon will produce a uniformly distributed upward load equal to

$$w_p = \frac{8Py}{l^2} \tag{19.33}$$

where P = magnitude of prestress force
y = maximum sag of tendon measured with respect to the chord between its end points
l = span length

If the downward load exactly equals the upward load from the tendon, these two loads cancel and no bending stress is produced, as shown in Fig. 19.20*b*. The bending stresses due to prestress eccentricity are equal and opposite to the bending stresses resulting from the external load. The net resulting stress is uniform compression f_a equal to that produced by the axial force $P \cos \cdot$. Excluding consideration of time-dependent effects, the beam would show no vertical deflection.

If the live load is removed or increased, then bending stresses and deflections will result because of the *unbalanced* portion of the load. Stresses resulting from this differential loading must be calculated and superimposed on the axial compression to obtain the net stresses for the unbalanced state. Referring to Fig. 19.20*c*, the bending stresses f_b' resulting from removal of the partial live loading are superimposed on the uniform compressive stress f_a, resulting from the combination of eccentric prestress force and full balanced load to produce the final stress distribution shown.

Loads other than uniformly distributed would lead naturally to the selection of other tendon configurations. For example, if the external load consisted of a single concentration at midspan, a deflected tendon such as that of Fig. 19.2*a* would be chosen, with maximum eccentricity at midspan, varying linearly to zero eccentricity at the supports. A third-point loading would lead the designer to select a tendon deflected at the third points. A uniformly loaded cantilever beam would best be stressed using a tendon in which the eccentricity varied parabolically, from zero at the free end to y at the fixed support, in which case the upward reaction of the tendon would be

$$w_p = \frac{2Py}{l^2} \tag{19.34}$$

It should be clear that, for simple spans designed by the load-balancing concept, it is necessary for the tendon to have zero eccentricity at the supports because the moment due to superimposed loads is zero there. Any tendon eccentricity would produce an unbalanced moment (in itself an equivalent load) equal to the horizontal component of the prestress force times its eccentricity. At the simply supported ends, the requirement of zero eccentricity must be retained.

In practice, the load-balancing method of design starts with selection of a trial beam cross section, based on experience and judgment. An appropriate span-depth ratio is often applied. The tendon profile is selected using the maximum available eccentricity, and the prestress force is calculated. The trial design may then be checked to ensure that concrete stresses are within the allowable limits should the live load be totally absent or fully in place, when bending stresses will be superimposed on the axial compressive stresses. There is no assurance that the section will be adequate for these load stages, nor that adequate strength will be provided should the member be overloaded. Revision may be necessary.

It should further be observed that obtaining a uniform compressive concrete stress at the balanced load stage does not ensure that the member will have zero deflection at this stage. The reason for this is that the uniform stress distribution is made up of two parts: that from the eccentric prestress force and that from the external loads. The prestress force varies with time because of shrinkage, creep, and relaxation, changing the vertical deflection associated with the prestress force. Concurrently, the beam will experience creep deflection under the combined effects of the diminishing prestress force and the external loads, a part of which may be sustained and a part of which may be short-term. However, if load balancing is carried out based on the effective prestress force P_e plus self-weight and external dead load only, the result may be near-zero deflection for that combination.

The load-balancing method provides the engineer with a useful tool. For simple spans, it leads the designer to choose a sensible tendon profile and focuses attention very early on the matter of deflection. But the most important advantages become evident in the design of indeterminate prestressed members, including both continuous beams and two-way slabs. For such cases, at least for one unique loading, the member carries only axial compression but no bending. This greatly simplifies the analysis.

EXAMPLE 19.5

Beam design initiating with load balancing. A post-tensioned beam is to be designed to carry a uniformly distributed load over a 30 ft span, as shown in Fig. 19.21. In addition to its own weight, it must carry a dead load of 150 lb/ft and a service live load of 600 lb/ft. Concrete strength of 4000 psi will be attained at 28 days; at the time of transfer of the prestress force, the strength will be 3000 psi. Prestress loss may be assumed at 20 percent of P_i. On the basis that about one-quarter of the live load will be sustained over a substantial time period, k_b of 0.25 will be used in determining the balanced load.

SOLUTION. On the basis of an arbitrarily chosen span-depth ratio of 18, a 20 in. deep, 10 in. wide trial section is selected. The calculated self-weight of the beam is 208 lb/ft and the selected load to be balanced is

$$w_{bal} = w_o + w_d + k_b w_l = 208 + 150 + 150 = 508 \text{ lb/ft}$$

Based on a minimum concrete cover from the steel centroid to the bottom face of the beam of 4 in., the maximum eccentricity that can be used for the 20 in. trial section is 6 in. A parabolic tendon will be used to produce a uniformly distributed upward tendon load. To equil-

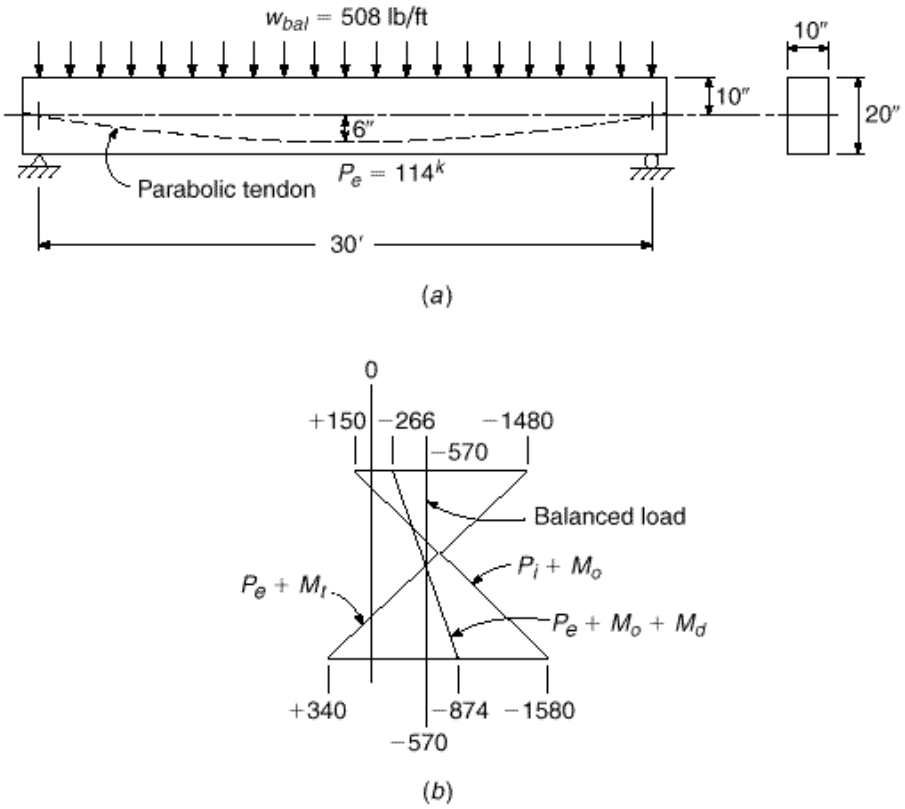

FIGURE 19.21
Example of design by load balancing: (*a*) beam profile and cross section; (*b*) flexural stresses at maximum moment section (psi).

ibrate the sustained downward loading, the prestress force P_e after losses, from Eq. (19.33), should be

$$P_e = \frac{w_{bal} l^2}{8y} = \frac{508 \times 900}{8 \times 0.5} = 114{,}000 \text{ lb}$$

and the corresponding initial prestress force is

$$P_i = \frac{P_e}{R} = \frac{114{,}000}{0.8} = 143{,}000 \text{ lb}$$

For the balanced load stage, the concrete will be subjected to a uniform compressive stress of

$$f_{bal} = \frac{114{,}000}{200} = -570 \text{ psi}$$

as shown in Fig. 19.21*b*. Should the partial live load of 150 lb/ft be removed, the stresses to be superimposed on f_{bal} result from a net *upward* load of 150 lb/ft. The section modulus for the trial beam is 667 in^3 and

$$M_{unbal} = 150 \times \frac{900}{8} = 16{,}900 \text{ ft-lb}$$

Hence, the unbalanced bending stresses at the top and bottom faces are

$$f_{unbal} = 16{,}900 \times \frac{12}{667} = 304 \text{ psi}$$

Thus, the net stresses are

$$f_1 = -570 + 304 = -266 \text{ psi}$$
$$f_2 = -570 - 304 = -874 \text{ psi}$$

Similarly, if the *full* live load should act, the stresses to be superimposed are those resulting from a net *downward* load of 450 lb/ft. The resulting stresses in the concrete at full service load are

$$f_1 = -570 - 910 = -1480 \text{ psi}$$
$$f_2 = -570 + 910 = +340 \text{ psi}$$

Stresses in the concrete with live load absent and live load fully in place are shown in Fig. 19.21*b*.

It is also necessary to investigate the stresses in the initial unloaded stage, when the member is subjected to P_i plus moment due to its own weight.

$$M_o = 208 \times \frac{900}{8} = 23{,}400 \text{ ft-lb}$$

Hence, in the initial stage:

$$f_1 = -\frac{143{,}000}{200} \cdot 1 - \frac{6 \times 10}{33.35} \cdot - \frac{23{,}400 \times 12}{667} = +150 \text{ psi}$$

$$f_2 = -\frac{143{,}000}{200} \cdot 1 + \frac{6 \times 10}{33.35} \cdot + \frac{23{,}400 \times 12}{667} = -1580 \text{ psi}$$

The stresses in the unloaded and full service load stages must be checked against these permitted by the ACI Code. With $f'_c = 4000$ psi and $f'_{ci} = 3000$ psi, the stresses permitted for a Class U member are:

$$f_{ti} = +165 \text{ psi} \qquad f_{ts} = +474 \text{ psi}$$
$$f_{ci} = -1800 \text{ psi} \qquad f_{cs} = -2400 \text{ psi}$$

The actual stresses, shown in Fig. 19.21*b*, are within these limits and acceptably close, and no revision will be made in the trial 10 × 20 in. cross section on the basis of stress limits.

The flexural strength of the members must now be checked, to ensure that an adequate margin of safety against collapse has been provided. The required P_i of 143,000 lb will be provided using Grade 270 strand, with $f_{pu} = 270{,}000$ psi and $f_{py} = 243{,}000$ psi. Referring to Section 19.4, the initial stress immediately after transfer must not exceed $0.74 \times 270{,}000 = 200{,}000$ psi, or $0.82 \times 243{,}000 = 199{,}000$ psi, which controls in this case. Accordingly, the required area of tendon steel is

$$A_{ps} = 143{,}000 \cdot 199{,}000 = 0.72 \text{ in}^2$$

This will be provided using five $\frac{1}{2}$ in. strands, giving an actual area of 0.765 in^2 (Table A.15). The resulting stresses at the initial and final stages are

$$f_{pi} = \frac{143{,}000}{0.765} = 187{,}000 \text{ psi}$$

$$f_{pe} = \frac{114{,}000}{0.765} = 149{,}000 \text{ psi}$$

Using the ACI approximate equation for steel stress at failure [see Eq. (19.6)], with $\cdot_p = 0.765 \cdot 160 = 0.0048$, and $\cdot_p = 0.40$ for the ordinary Grade 270 tendons, the stress f_{ps} is given by

$$f_{ps} = f_{pu} \cdot 1 - \frac{\cdot_p}{\cdot_1} \frac{\cdot_p f_{pu}}{f_c} \cdot$$

$$= 270 \cdot 1 - \frac{0.40}{0.85} \frac{0.0048 \times 270}{4} \cdot$$

$$= 229 \text{ ksi}$$

Then,

$$a = \frac{A_{ps} f_{ps}}{0.85 f_c b}$$

$$= \frac{0.765 \times 229}{0.85 \times 4 \times 10} = 5.15 \text{ in.}$$

$$c = \frac{5.15}{0.85} = 6.06$$

$$\frac{c}{d_t} = \frac{6.06}{16} = 0.379$$

This exceeds $c \cdot d_t = 0.375$, reducing $\cdot$ to 0.89. The nominal flexural strength is

$$M_n = A_{ps} f_{ps} \cdot d - \frac{a}{2} \cdot = 0.765 \times 229{,}000 \cdot 16 - \frac{5.15}{2} \cdot \frac{1}{12}$$

$$= 196{,}000 \text{ ft-lb}$$

and the design strength with $\cdot = 0.89$ is

$$\cdot M_n = 0.89 \times 196{,}000 = 174{,}000 \text{ ft-lb}$$

It will be recalled that the ACI load factors with respect to dead and live loads are, respectively, 1.2 and 1.6. Calculating the factored load,

$$w_u = 1.2 \cdot 208 + 150 \cdot + 1.6 \cdot 600 \cdot = 1390 \text{ lb} \cdot \text{ft}$$

$$M_u = \frac{1390 \cdot 900 \cdot}{8} = 156{,}000 \text{ ft-lb}$$

Thus, $\cdot M_n > M_u$, and the design is judged satisfactory.

19.13 Loss of Prestress

As discussed in Section 19.6, the initial prestress force P_i immediately after transfer is less than the jacking force P_j because of elastic shortening of the concrete, slip at the anchorages, and frictional losses along the tendons. The force is reduced further, after a period of many months or even years, due to length changes resulting from shrinkage and creep of the concrete and relaxation of the highly stressed steel; eventually it attains its effective value P_e. In the preceding sections of this chapter, losses were accounted for, making use of an assumed effectiveness ratio $R = P_e/P_i$. Losses have no effect on the nominal strength of a member with bonded tendons, but overestimation or underestimation of losses may have a pronounced effect on service conditions including camber, deflection, and cracking.

The estimation of losses can be made on several different levels. Lump sum losses, used in the early development of prestressed concrete are now considered obsolete. Values of R, based on detailed calculations and verified in field applications are used in design offices, as are tables of individual loss contributions. For cases where greater accuracy is required, it is necessary to estimate the separate losses, taking account of the conditions of member geometry, material properties, and construction methods that apply. Accuracy of loss estimation can be improved still further by accounting for the interdependence of time-dependent losses, using the summation of losses in a sequence of discrete time steps. These methods will be discussed briefly in the following paragraphs.

a. Lump-Sum Estimates of Losses

It was recognized very early in the development of prestressed concrete that there was a need for approximate expressions to be used to estimate prestress losses in design. Many thousands of successful prestressed structures have been built based on such estimates, and where member sizes, spans, materials, construction procedures, amount of prestress force, and environmental conditions are not out of the ordinary, this approach is satisfactory. For such conditions, the American Association of State Highway and Transportation Officials (AASHTO, Ref. 19.17) has recommended the values in Table 19.3 for preliminary design or for certain controlled precasting conditions. It should be noted that losses due to friction must be added to these values for post-tensioned members. These may be calculated separately by the equations of Section 19.13b below.

The AASHTO recommended losses of Table 19.3 include losses due to elastic shortening, creep, shrinkage, and relaxation (see Section 19.13b). Thus for comparison with R values for estimating losses, such as were employed for the preceding examples, which included only the time-dependent losses due to shrinkage, creep, and relaxation, elastic shortening losses should be estimated by the methods discussed in Section 19.13b and deducted from the total.

b. Estimate of Separate Losses

For most designs, a separate estimate of individual losses is made. Such an analysis is complicated by the interdependence of time-dependent losses. For example, the relaxation of stress in the tendons is affected by length changes due to creep of concrete. Rate of creep, in turn, is altered by change in tendon stress. In the following six subsections,

TABLE 19.3
Estimate of prestress losses

Type of Beam Section	Level	Wires or Strands with = 235, 250, or 270 ksi
Rectangular beams, solid slabs	Upper bound	33.0 ksi
	Average	30.0 ksi
Box girder	Upper bound	25.0 ksi
	Average	23.0 ksi
I girder	Average	$33.0[1 - 0.15(f'_c - 6.0)\cdot 6.0] + 6.0$
Single T, double T,	Upper bound	$39.0[1 - 0.15(f'_c - 6.0)\cdot 6.0] + 6.0$
hollow core and voided slab	Average	$39.0[1 - 0.15(f'_c - 6.0)\cdot 6.0] + 6.0$

[a] Values are for fully prestressed beams; reductions are allowed for partial prestress.
Losses due to friction are excluded. Friction losses should be computed according to Section 19.13b.
For low-relaxation strands, the values specified may be reduced by 4.0 ksi for box girders; 6.0 ksi for rectangular beams, solid slabs, and I girders; and 8.0 ksi for single T's, double T's, hollow core and voided slabs.

Source: Adapted from Ref. 19.17.

losses are treated as if they occurred independently, although certain arbitrary adjustments are included to account for the interdependence of time-dependent losses. If greater refinement is necessary, a step-by-step approach, like that mentioned in Section 19.13c, may be used (see also Refs. 19.18 and 19.19).

(1) SLIP AT THE ANCHORAGES As the load is transferred to the anchorage device in post-tensioned construction, a slight inward movement of the tendon will occur as the wedges seat themselves and as the anchorage itself deforms under stress. The amount of movement will vary greatly, depending on the type of anchorage and on construction techniques. The amount of movement due to seating and stress deformation associated with any particular type of anchorage is best established by test. Once this amount ΔL is determined, the stress loss is easily calculated from

$$f_{s,slip} = \frac{\Delta L}{L} E_s \tag{19.35}$$

It is significant to note that the amount of slip is nearly independent of the cable length. For this reason, the stress loss will be large for short tendons and relatively small for long tendons. The practical consequence of this is that it is most difficult to post-tension short tendons with any degree of accuracy.

(2) ELASTIC SHORTENING OF THE CONCRETE In pretensioned members, as the tendon force is transferred from the fixed abutments to the concrete beam, elastic instantaneous compressive strain will take place in the concrete, tending to reduce the stress in the bonded prestressing steel. The steel stress loss is

$$f_{s,elastic} = E_s \frac{f_c}{E_c} = n f_c \tag{19.36}$$

where f_c is the concrete stress at the level of the steel centroid immediately after prestress is applied:

$$f_c = -\frac{P_i}{A_c}\left(1 + \frac{e^2}{r^2}\right) + \frac{M_0 e}{I_c} \tag{19.37}$$

If the tendons are placed with significantly different effective depths, the stress loss in each should be calculated separately.

In computing f_c by Eq. (19.37), the prestress force used should be that after the losses being calculated have occurred. It is usually adequate to estimate this as about 10 percent less than P_j.

In post-tensioned members, if all of the strands are tensioned at one time, there will be no loss due to elastic shortening, because this shortening will occur as the jacking force is applied and before the prestressing force is measured. On the other hand, if various strands are tensioned sequentially, the stress loss in each strand will vary, being a maximum in the first strand tensioned and zero in the last strand. In most cases, it is sufficiently accurate to calculate the loss in the first strand and to apply one-half that value to all strands.

(3) FRICTIONAL LOSSES Losses due to friction, as the tendon is stressed in post-tensioned members, are usually separated for convenience into two parts: curvature friction and wobble friction. The first is due to intentional bends in the tendon profile as specified and the second to the unintentional variation of the tendon from its intended profile. It is apparent that even a "straight" tendon duct will have some unintentional misalignment so that wobble friction must always be considered in post-tensioned work. Usually, curvature friction must be considered as well. The force at the jacking end of the tendon P_o, required to produce the force P_x at any point x along the tendon, can be found from the expression

$$P_o = P_x e^{Kl_x + \cdot} \qquad (19.38a)$$

where e = base of natural logarithms
l_x = tendon length from jacking end to point x
$\cdot$ = angular change of tendon from jacking end to point x, radians
K = wobble friction coefficient, lb/lb per ft
$\cdot$ = curvature friction coefficient

There has been much research on frictional losses in prestressed construction, particularly with regard to the values of K and $\cdot$. These vary appreciably, depending on construction methods and materials used. The values in Table 19.4, from ACI Commentary R18.6, may be used as a guide.

TABLE 19.4
Friction coefficients for post-tensioned tendons

Type of Tendon	Wobble Coefficient $\cdot$, per ft	Curvature Coefficient $\cdot$
Grouted tendons in metal sheathing		
Wire tendons	0.0010–0.0015	0.15–0.25
High-strength bars	0.0001–0.0006	0.08–0.30
Seven-wire strand	0.0005–0.0020	0.15–0.25
Unbonded tendons		
Mastic-coated wire tendons	0.0010–0.0020	0.05–0.15
Mastic-coated seven-wire strand	0.0010–0.0020	0.05–0.15
Pregreased wire tendons	0.0003–0.0020	0.05–0.15
Pregreased seven-wire strand	0.0003–0.0020	0.05–0.15

If one accepts the approximation that the normal pressure on the duct causing the frictional force results from the undiminished initial tension all the way around the curve, the following simplified expression for loss in tension is obtained:

$$P_o = P_x \cdot 1 + Kl_x + \cdots \qquad (19.38b)$$

where $\cdot$ is the angle between the tangents at the ends. The ACI Code permits the use of the simplified form, if the value of $Kl_x + \cdots$ is not greater than 0.3.

The loss of prestress for the entire tendon length can be computed by segments, with each segment assumed to consist of either a circular arc or a length of tangent.

(4) CREEP OF CONCRETE Shortening of concrete under sustained load has been discussed in Section 2.8. It can be expressed in terms of the creep coefficient C_c. Creep shortening may be several times the initial elastic shortening, and it is evident that it will result in loss of prestress force. The stress loss can be calculated from

$$\cdot f_{s,creep} = C_c n f_c \qquad (19.39)$$

Ultimate values of C_c for different concrete strengths for average conditions of humidity C_{cu} are given in Table 2.1.

In Eq. (19.39), the concrete stress f_c to be used is that at the level of the steel centroid, when the eccentric prestress force plus all sustained loads are acting. Equation (19.37) can be used, except that the moment M_o should be replaced by the moment due to *all* dead loads plus that due to any portion of the live load that may be considered sustained.

It should be noted that the prestress force causing creep is not constant but diminishes with the passage of time due to relaxation of the steel, shrinkage of the concrete, and length changes associated with creep itself. To account for this, it is recommended that the prestress force causing creep be assumed at 10 percent less than the initial value P_i.

(5) SHRINKAGE OF CONCRETE It is apparent that a decrease in the length of a member due to shrinkage of the concrete will be just as detrimental as length changes due to stress, creep, or other causes. As discussed in Section 2.11, the shrinkage strain $\cdot_{sh}$ may vary between about 0.0004 and 0.0008. A typical value of 0.0006 may be used in lieu of specific data. The steel stress loss resulting from shrinkage is

$$\cdot f_{s,shrink} = \cdot_{sh} E_s \qquad (19.40)$$

Only that part of the shrinkage that occurs after transfer of prestress force to the concrete need be considered. For pretensioned members, transfer commonly takes place just 18 hours after placing the concrete, and nearly all the shrinkage takes place after that time. However, post-tensioned members are seldom stressed at an age earlier than 7 days and often much later than that. About 15 percent of ultimate shrinkage may occur within 7 days, under typical conditions, and about 40 percent by the age of 28 days.

(6) RELAXATION OF STEEL The phenomenon of relaxation, similar to creep, was discussed in Section 2.16c. Loss of stress due to relaxation will vary depending upon the stress in the steel, and may be estimated using Eqs. (2.11) and (2.12). To allow for the gradual reduction of steel stress resulting from the combined effects of creep, shrinkage, and relaxation, the relaxation calculation can be based on a prestress force 10 percent less than P_i.

It is interesting to observe that the largest part of the relaxation loss occurs shortly after the steel is stretched. For stresses of $0.80 f_{pu}$ and higher, even a very short period of loading will produce substantial relaxation, and this in turn will reduce the

relaxation that will occur later at a lower stress level. The relaxation rate can thus be artificially accelerated by temporary overtensioning. This technique is the basis for producing low-relaxation steel.

c. Loss Estimation by the Time-Step Method

The loss calculations of the preceding paragraphs recognized the interdependence of creep, shrinkage, and relaxation losses in an approximate way, by an arbitrary reduction of 10 percent of the initial prestress force P_i to obtain the force for which creep and relaxation losses were calculated. For cases requiring greater accuracy, losses can be calculated for discrete time steps over the period of interest. The prestress force causing losses during any time step is taken equal to the value at the end of the preceding time step, accounting for losses due to all causes up to that time. Accuracy can be improved to any desired degree by reducing the length and increasing the number of time steps.

A step-by-step method developed by the Committee on Prestress Losses of the Prestressed Concrete Institute uses only a small number of time steps and is adequate for ordinary cases (Ref. 19.18).

19.14 Shear, Diagonal Tension, and Web Reinforcement

In prestressed concrete beams at service load, there are two factors that greatly reduce the intensity of diagonal tensile stresses, compared with stresses that would exist if no prestress force were present. The first of these results from the combination of longitudinal compressive stress and shearing stress. An ordinary tensile-reinforced-concrete beam under load is shown in Fig. 19.22*a*. The stresses acting on a small element of the beam taken near the neutral axis and near the support are shown in (*b*). It is found by

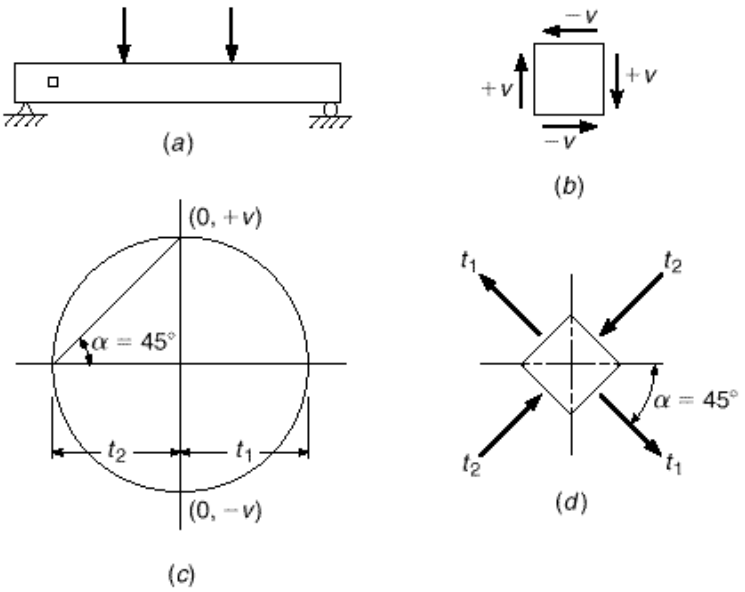

FIGURE 19.22
Principal stress analysis for an ordinary reinforced concrete beam.

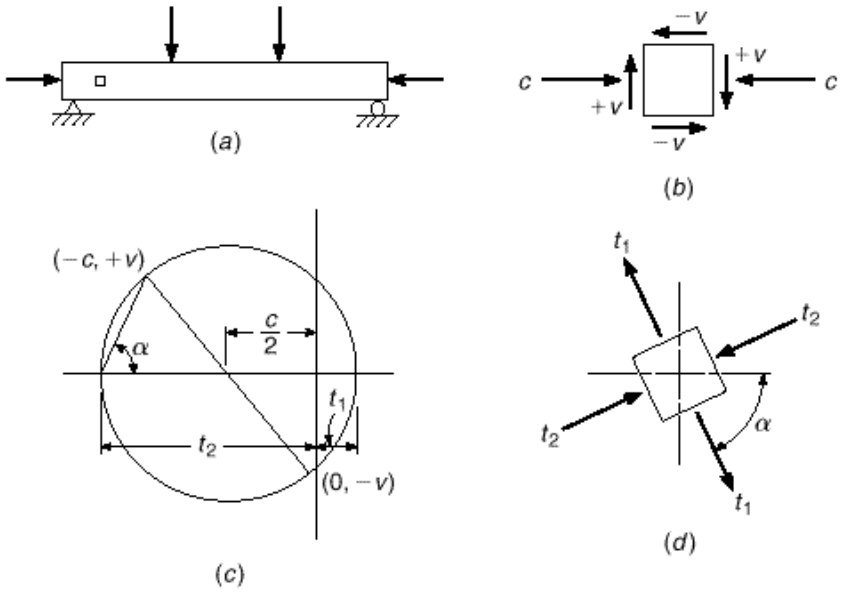

FIGURE 19.23
Principal stress analysis for a prestressed concrete beam.

means of Mohr's circle of stress (*c*) that the principal stresses act at 45° to the axis of the beam (*d*) and are numerically equal to the shear stress intensity; thus

$$t_1 = t_2 = v \tag{a}$$

Now suppose that the same beam, with the same loads, is subjected to a precompression stress in the amount *c*, as shown in Fig. 19.23*a* and *b*. From Mohr's circle (Fig. 19.23*c*), the principal tensile stress is

$$t_1 = -\frac{c}{2} + \sqrt{v^2 + \left(\frac{c}{2}\right)^2} \tag{b}$$

and the direction of the principal tension with respect to the beam axis is

$$\tan 2\alpha = \frac{2v}{c} \tag{c}$$

as shown in Fig. 19.23*d*.

Comparison of Eq. (*a*) with Eq. (*b*) and Fig. 19.22*c* with Fig. 19.23*c* shows that, with the same shear stress intensity, the principal tension in the prestressed beam is much reduced.

The second factor working to reduce the intensity of the diagonal tension at service loads results from the slope of the tendons. Normally, this slope is such as to produce a shear due to the prestress force that is opposite in direction to the load-imposed shear. The magnitude of this *countershear* is $V_p = P_e \sin \alpha$, where α is the slope of the tendon at the section considered (see Fig. 19.8).

It is important to note, however, that in spite of these characteristics of prestressed beams at service loads, an investigation of diagonal tensile stresses at service loads does not ensure an adequate margin of safety against failure. In Fig. 19.23*c*, it is evident that a relatively small decrease in compressive stress and increase in shear stress, which may occur when the beam is overloaded, will produce a disproportionately large increase in the resulting principal tension. In addition to this effect, if the countershear of inclined tendons is used to reduce design shear, its contribution does

not increase directly with load, but much more slowly (see Section 19.7). Consequently, a small increase in total shear may produce a large increase in the net shear for which the beam must be designed. For these two reasons, it is necessary to base design for diagonal tension in prestressed beams on conditions at factored load rather than at service load. The study of principal stresses in the uncracked prestressed beam is significant only in predicting the load at which the first diagonal crack forms.

At loads near failure, a prestressed beam is usually extensively cracked and behaves much like an ordinary reinforced concrete beam. Accordingly, many of the procedures and equations developed in Section 4.5 for the design of web reinforcement for nonprestressed beams can be applied to prestressed beams also. Shear design is based on the relation

$$V_u \leq \cdot\ V_n \tag{19.41}$$

where V_u is the total shear force applied to the section at factored loads and V_n is the nominal shear strength, equal to the sum of the contributions of the concrete V_c and web reinforcement V_s:

$$V_n = V_c + V_s \tag{19.42}$$

The strength reduction factor $\cdot$ is equal to 0.75 for shear.

In computing the factored load shear V_u, the first critical section is assumed to be at a distance $h \cdot 2$ from the face of a support, and sections located a distance less than $h \cdot 2$ are designed for the shear computed at $h \cdot 2$.

The shear force V_c resisted by the concrete after cracking has occurred is taken equal to the shear that causes the first diagonal crack. Two types of diagonal cracks have been observed in tests of prestressed concrete beams:

1. **Flexure-shear cracks,** occurring at nominal shear V_{ci}, start as nearly vertical flexural cracks at the tension face of the beam, then spread diagonally upward (under the influence of diagonal tension) toward the compression face. These are common in beams with a low value of prestress force.
2. **Web-shear cracks,** occurring at nominal shear V_{cw}, start in the web due to high diagonal tension, then spread diagonally both upward and downward. These are often found in beams with thin webs with high prestress force.

On the basis of extensive tests, it was established that the shear causing flexure shear cracking can be found using the expression

$$V_{ci} = 0.6 \cdot \sqrt{f'_c} b_w d + V_{cr,o+d+l} \tag{a}$$

where $V_{cr,o+d+l}$ is the shear force, due to total load, at which the flexural crack forms at the section considered, and $0.6 \cdot \sqrt{f'_c} b_w d$ represents an additional shear force required to transform the flexural crack into an inclined crack.

While self-weight is generally uniformly distributed, the superimposed dead and live loads may have any distribution. Consequently, it is convenient to separate the total shear into V_o caused by the beam self-weight (without load factor) and V_{cr}, the additional shear force, due to superimposed dead and live loads, corresponding to flexural cracking. Thus,

$$V_{ci} = 0.6 \cdot \sqrt{f'_c} b_w d + V_o + V_{cr} \tag{b}$$

The shear V_{cr} due to superimposed loads can then be found conveniently from

$$V_{cr} = \frac{V_{d+l}}{M_{d+l}} M_{cr} \tag{c}$$

where $V_{d+l} \cdot M_{d+l}$, the ratio of superimposed dead and live load shear to moment, remains constant as the load increases to the cracking load, and

$$M_{cr} = \frac{I_c}{c_2} \cdot 6 \cdot \sqrt{f'_c} + f_{2pe} - f_{2o} \cdot \tag{19.43}$$

where c_2 = distance from concrete centroid to tension face
f_{2pe} = compressive stress at tension face resulting from effective prestress force alone
f_{2o} = bottom-fiber stress due to beam self-weight (unfactored)†

The first term in the parentheses is a conservative estimate of the modulus of rupture. The bottom-fiber stress due to self-weight is subtracted here because self-weight is considered separately in Eq. (*b*). Thus, Eq. (*b*) becomes

$$V_{ci} = 0.6 \cdot \sqrt{f'_c} b_w d + V_o + \frac{V_{d+l}}{M_{d+l}} M_{cr} \tag{19.44}$$

Tests indicate that V_{ci} need not be taken less than $1.7 \cdot \sqrt{f'_c} b_w d$. The value of d need not be taken less than $0.80h$ for this and all other equations relating to shear, according to the ACI Code, unless specifically noted otherwise. Additionally, the values V_{d+l} and M_{d+l} should be computed for the load combination causing the maximum moment in the section. Because V_{d+l} is the incremental load above the beam self-weight, the ACI uses the notation $V_l M_{cr} \cdot M_{max}$, noting that M_{cr} comes from Eq. (19.43).

The shear force causing web-shear cracking can be found from an exact principal stress calculation, in which the principal tensile stress is set equal to the direct tensile capacity of the concrete (conservatively taken equal to $4 \cdot \sqrt{f'_c}$ according to the ACI Code). Alternatively, the ACI Code permits use of the approximate expression

$$V_{cw} = \cdot 3.5 \cdot \sqrt{f'_c} + 0.3 f_{pc} \cdot b_w d + V_p \tag{19.45}$$

in which f_{pc} is the compressive stress in the concrete, after losses, at the centroid of the concrete section (or at the junction of the web and the flange when the centroid lies in the flange) and V_p is the vertical component of the effective prestress force. In a pretensioned beam, the $0.3f_{pc}$ contribution to V_{cw} should be adjusted from zero at the beam end to its full value one transfer length (see Section 19.15b) in from the end of the beam.

After V_{ci} and V_{cw} have been calculated, then V_c, the shear resistance provided by the concrete, is taken equal to the smaller of the two values.

Calculating M_{cr}, V_{ci}, and V_{cw} for a prestressed beam is a tedious matter because many of the parameters vary along the member axis. For hand calculations, the required quantities may be found at discrete intervals along the span, such as at $l \cdot 2$, $l \cdot 3$, $l \cdot 6$, and at $h \cdot 2$ from the support face, and stirrups spaced accordingly, or computer spreadsheets may be used.

To shorten the calculation required, the ACI Code includes, as a conservative alternative to the above procedure, an equation for finding the concrete shear resistance V_c directly:

$$V_c = \cdot 0.6 \cdot \sqrt{f'_c} + 700 \frac{V_u d}{M_u} \cdot b_w d \tag{19.46}$$

in which M_u is the bending moment occurring simultaneously with shear force V_u, but $V_u d \cdot M_u$ is not to be taken greater than 1.0. When this equation is used, V_c need not be

† All stresses are used with absolute value here, consistent with ACI convention.

taken less than $2\cdot\sqrt{f'_c}b_w d$ and must not be taken greater than $5\cdot\sqrt{f'_c}b_w d$. While Eq. (19.46) is temptingly easy to use and may be adequate for uniformly loaded members of minor importance, its use is apt to result in highly uneconomical designs for I beams with medium and long spans and for composite construction (Ref. 19.20).

When shear reinforcement perpendicular to the axis of the beam is used, its contribution to shear strength of a prestressed beam is

$$V_s = \frac{A_v f_y d}{s} \tag{19.47}$$

the same as for a nonprestressed member. According to the ACI Code, the value of V_s must not be taken greater than $8\cdot\sqrt{f'_c}b_w d$.

The total nominal shear strength V_n is found by summing the contributions of the concrete and steel, as indicated by Eq. (19.42):

$$V_n = V_c + \frac{A_v f_y d}{s} \tag{19.48}$$

Then, from Eq. (19.41),

$$V_u = \cdot\, V_n = \cdot\,\cdot V_c + V_s\cdot$$

from which

$$V_u = \cdot\,\cdot\, V_c + \frac{A_v f_y d}{s}\cdot \tag{19.49}$$

The required cross-sectional area of one stirrup A_v can be calculated by suitable transposition of Eq. (19.49).

$$A_v = \frac{\cdot V_u - \cdot\, V_c\cdot s}{\cdot\, f_y d} \tag{19.50}$$

Normally, in practical design, the engineer will select a trial stirrup size, for which the required spacing is found. Thus, a more convenient form of the last equation is

$$s = \frac{\cdot\, A_v f_y d}{V_u - \cdot\, V_c} \tag{19.51}$$

A minimum area of shear reinforcement is required in all prestressed concrete members where the total factored shear force is greater than one-half the design shear strength provided by the concrete $\cdot\, V_c$. Exceptions are made for slabs and footings, concrete-joist floor construction, and certain very shallow beams, according to the ACI Code. The minimum area of shear reinforcement to be provided in all other cases is equal to the smaller of

$$A_v = 0.75\cdot\sqrt{f'_c}\frac{b_w s}{f_y} \le 50\frac{b_w s}{f_y} \tag{19.52}$$

and

$$A_v = \frac{A_{ps}}{80}\frac{f_{pu}}{f_y}\frac{s}{d}\cdot\sqrt{\frac{d}{b_w}} \tag{19.53}$$

in which A_{ps} is the cross-sectional area of the prestressing steel, f_{pu} is the tensile strength of the prestressing steel, and all other terms are as defined above.

The ACI Code contains certain restrictions on the maximum spacing of web reinforcement to ensure that any potential diagonal crack will be crossed by at least a minimum amount of web steel. For prestressed members, this maximum spacing is not to exceed the smaller of $0.75h$ or 24 in. If the value V_s exceeds $4\sqrt{f'_c}\,b_w d$, these limits are reduced by half.

EXAMPLE 19.6

The unsymmetrical I beam shown in Fig. 19.24 carries an effective prestress force of 288 kips and supports a superimposed dead load of 345 lb/ft and service live load of 900 lb/ft, in addition to its own weight of 255 lb/ft, on a 50 ft simple span. At the maximum moment section, the effective depth to the main steel is 24.5 in. (eccentricity 11.4 in.). The strands are deflected upward starting 15 ft from the support, and eccentricity is reduced linearly to zero at the support. If concrete with $f'_c = 5000$ psi and stirrups with $f_y = 60{,}000$ psi are used, and if the prestressed strands have strength $f_{pu} = 270$ ksi, what is the required stirrup spacing at a point 10 ft from the support?

SOLUTION. For a cross section with the given dimensions, it is easily confirmed that $I_c = 24{,}200$ in^4, $A_c = 245$ in^2, and $r^2 = I_c/A_c = 99$ in^2. At a distance 10 ft from the support centerline, the tendon eccentricity is

$$e = 11.4 \times \frac{10}{15} = 7.6 \text{ in.}$$

corresponding to an effective depth d from the compression face of 20.7 in. According to the ACI Code, the larger value of $d = 0.80 \times 29 = 23.2$ in. will be used. Calculation of V_{ci} is based on Eqs. (19.43) and (19.44). The bottom-fiber stress due to effective prestress acting alone is

$$f_{2pe} = -\frac{P_e}{A_c}\left(1 + \frac{ec_2}{r^2}\right) = -\frac{288{,}000}{245}\left(1 + \frac{7.6 \times 15.9}{99}\right) = -2600 \text{ psi}$$

The moment and shear at the section due to beam load alone are, respectively,

$$M_{o,10} = \frac{w_o x}{2}(l - x) = 0.255 \times 5 \times 40 = 51 \text{ ft-kips}$$

$$V_{o,10} = w_o\left(\frac{l}{2} - x\right) = 0.255 \times 15 = 3.8 \text{ kips}$$

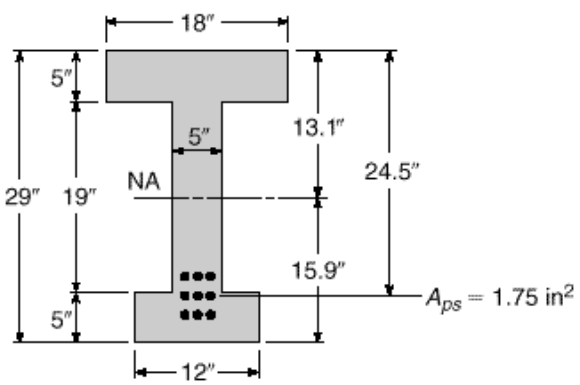

FIGURE 19.24
Post-tensioned beam in Example 19.6.

and the bottom fiber stress due to this load is

$$f_{2o} = \frac{51 \times 12{,}000 \times 15.9}{24{,}200} = 402 \text{ psi}$$

Then, from Eq. (19.43),

$$M_{cr} = \frac{24{,}200 \cdot 425 + 2600 - 402 \cdot}{15.9 \times 12} = 333{,}000 \text{ ft-lb}$$

The ratio of superimposed load shear to moment at the section is

$$\frac{V_{d+l}}{M_{d+l}} = \frac{l - 2x}{x \cdot l - x \cdot} = \frac{30}{400} = 0.075 \text{ ft}^{-1}$$

Equation (19.44) is then used to determine the shear force at which flexure-shear cracks can be expected to form.

$$V_{ci} = \cdot 0.6 \cdot \sqrt{5000} \cdot 5 \times 23.2 \cdot + 3800 + 0.075 \times 330{,}000 \cdot \times \frac{1}{1000} = 33.5 \text{ kips}$$

The lower limit of $1.7 \cdot \sqrt{5000} \cdot 5 \times 23.2 \cdot \cdot 1000 = 13.9$ kips does not control.

Calculation of V_{cw} is based on Eq. (19.45). The slope $\cdot$ of the tendons at the section under consideration is such that $\sin \cdot \approx \tan \cdot = 11.4 \cdot (15 \times 12) = 0.063$. Consequently, the vertical component of the effective prestress force is $V_p = 0.063 \times 288 = 18.1$ kips. The concrete compressive stress at the section centroid is

$$f_{pc} = \frac{288{,}000}{245} = 1170 \text{ psi}$$

Equation (19.45) can now be used to find the shear at which web-shear cracks should occur.

$$V_{cw} = \cdot \cdot 3.5 \cdot \sqrt{5000} + 0.3 \times 1170 \cdot 5 \times 23.2 + 18{,}100 \cdot \times \frac{1}{1000} = 87.5 \text{ kips}$$

Thus, in the present case,

$$V_c = V_{ci} = 33.5 \text{ kips}$$

At the section considered, the total shear force at factored loads is

$$V_u = 1.2 \times 0.600 \times 15 + 1.6 \times 0.900 \times 15 = 32.4 \text{ kips}$$

When No. 3 (No. 10) U stirrups are used, for which $A_v = 2 \times 0.11 = 0.22$ in^2, the required spacing is found from Eq. (19.51) to be

$$s = \frac{0.75 \times 0.22 \times 60{,}000 \times 23.2}{32{,}400 - 0.75 \times 33{,}500} = 32 \text{ in.}$$

Equation (19.53) is then applied to establish a maximum spacing criterion.

$$0.22 = \frac{1.75}{80} \times \frac{270}{60} \times \frac{s}{23.2 \cdot} \sqrt{\frac{23.2}{5}} = 0.0091s$$

$$s = 24.1 \text{ in.}$$

The other criteria for maximum spacing, three-fourths $\times$ 29 = 22 in. and 24 in., however, control here. Open U stirrups will be used, at a spacing of 22 in.

For comparison, the concrete shear will be calculated on the basis of Eq. (19.46). The ratio $V_u \cdot M_u$ is 0.075, and

$$V_c = \cdot 0.6 \cdot \sqrt{5000} + 700 \times \frac{0.075}{12} \times 23.2 \cdot \cdot 5 \times 23.2 \cdot \times \frac{1}{1000} = 16.7 \text{ kips}$$

The lower and upper limits, $2\cdot\sqrt{5000}(5\times 23.2)\cdot 1000 = 16.4$ kips and $5\cdot\sqrt{5000}(5\times 23.2)\cdot 1000 = 41.0$ kips, do not control. Thus, on the basis of V_c obtained from Eq. (19.46), the required spacing of No. 3 (No. 10) U stirrups is

$$s = \frac{0.75 \times 0.22 \times 60{,}000 \times 23.2}{32{,}400 - 0.75 \times 16{,}700} = 11.6 \text{ in.}$$

For the present case, an I-section beam of intermediate span, nearly 2 times the web steel is required at the location investigated if the alternative expression giving V_c directly is used.

19.15 Bond Stress, Transfer Length, and Development Length

There are two separate sources of bond stress in prestressed concrete beams: (1) flexural bond, which exists in pretensioned construction between the tendons and the concrete and in grouted post-tensioned construction between the tendons and the grout and between the conduit (if any) and concrete, and (2) prestress transfer bond, generally applicable to pretensioned members only.

a. Flexural Bond

Flexural bond stresses arise due to the change in tension along the tendon resulting from differences in bending moment at adjacent sections. They are proportional to the rate of change of bending moment, hence to the shear force, at a given location along the span. Provided the concrete member is uncracked, flexural bond stress is very low. After cracking, it is higher by an order of magnitude. However, flexural bond stress need not be considered in designing prestressed concrete beams, provided that adequate end anchorage is furnished for the tendon, either in the form of mechanical anchorage (post-tensioning) or strand embedment (pretensioning).

b. Transfer Length and Development Length

For pretensioned beams, when the external jacking force is released, the prestressing force is transferred from the steel to the concrete near the ends of the member by bond, over a distance which is known as the *transfer length*. The transfer length depends upon a number of factors, including the steel stress, the configuration of the steel cross section (e.g., strands vs. wires), the condition of the surface of the steel, and the suddenness with which the jacking force is released. Based on tests of seven-wire prestressing strand (Ref. 19.21), the effective prestress f_{pe} in the steel may be assumed to act at a transfer length from the end of the member equal to

$$l_t = \frac{f_{pe}}{3}\, d_b \qquad (a)$$

where l_t = transfer length, in.
d_b = nominal strand diameter, in.
f_{pe} = effective prestress, ksi

The same tests indicate that the additional distance past the original transfer length necessary to develop the failure strength of the steel is closely represented by the expression

$$l_t = (f_{ps} - f_{pe})d_b \qquad (b)$$

where the quantity in parentheses is the stress increment above the effective prestress level, in ksi units, to reach the calculated steel stress at failure f_{ps}. Thus the total development length at failure is

$$l_d = l_t + l_t \qquad (c)$$

or

$$l_d = (f_{ps} - \frac{2}{3} f_{pe})\, d_b \qquad (19.54)$$

The ACI Code does not require that flexural bond stress be checked in either pretensioned or post-tensioned members, but for pretensioned strand it is required that the full development length, given by Eq. (19.54), be provided beyond the critical bending section. Investigation may be limited to those cross sections nearest each end of the member that are required to develop their full flexural strength under the specified factored load.

19.16 Anchorage Zone Design

In prestressed concrete beams, the prestressing force is introduced as a load concentration acting over a relatively small fraction of the total member depth. For post-tensioned beams with mechanical anchorage, the load is applied at the end face, while for pretensioned beams it is introduced somewhat more gradually over the transfer length. In either case, the compressive stress distribution in the concrete becomes linear, conforming to that dictated by the overall eccentricity of the applied forces, only after a distance from the end roughly equal to the depth of the beam.

This transition of longitudinal compressive stress, from concentrated to linearly distributed, produces transverse (vertical) tensile stresses that may lead to longitudinal cracking of the member. The pattern and magnitude of the concrete stresses depend on the location and distribution of the concentrated forces applied by the tendons. Numerous studies have been made using the methods of classical elasticity, photoelasticity, and finite element analysis, and typical results are given in Fig. 19.25. Here the beam is loaded uniformly over a height equal to $h/8$ at an eccentricity of $3h/8$. Contour lines are drawn through points of equal vertical tension, with coefficients expressing the ratio of vertical stress to average longitudinal compression. Typically, there are high *bursting stresses* along the axis of the load a short distance inside the end zone and high *spalling stresses* at the loaded face.

In many post-tensioned prestressed I beams, solid end blocks are provided, as shown in Fig. 19.26. While these are often necessary to accommodate end-anchorage hardware and supplemental reinforcement, they are of little use in reducing transverse tension or avoiding cracking.

Steel reinforcement for end-zone stresses may be in the form of vertical bars of relatively small diameter and close spacing and should be well anchored at the top and bottom of the member. Closed stirrups are commonly used, with auxiliary horizontal bars inside the 90° bends.

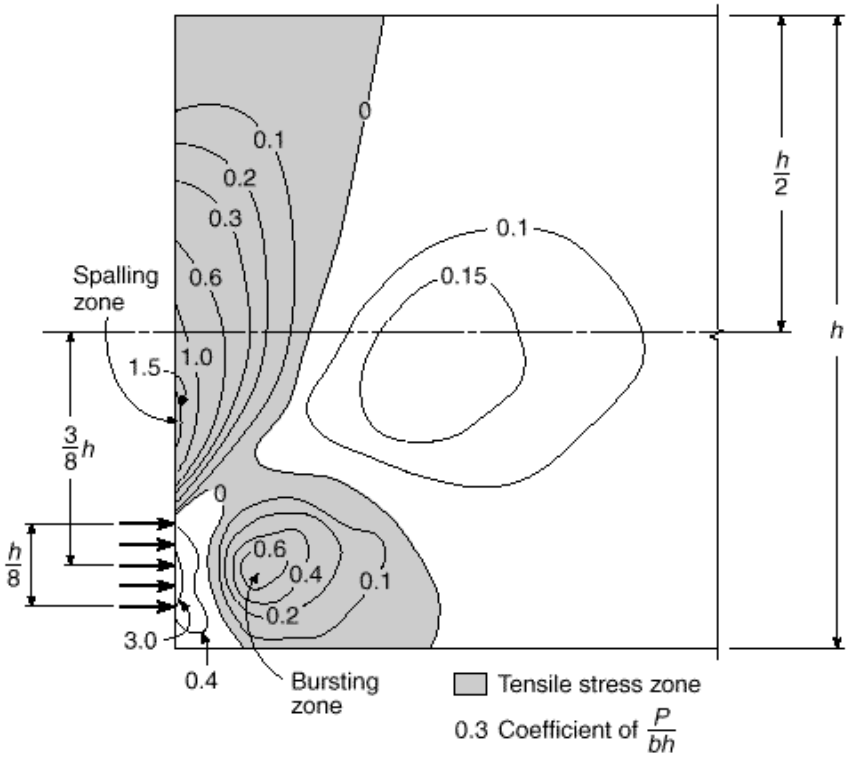

FIGURE 19.25
Contours of equal vertical stress. (*Adapted from Ref. 19.16.*)

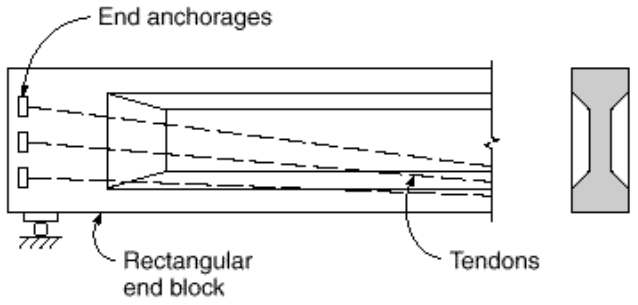

FIGURE 19.26
Post-tensioned I beam with rectangular end block.

Rational design of the reinforcement for end zones must recognize that horizontal cracking is likely. If adequate reinforcement is provided, so that the cracks are restricted to a few inches in length and to 0.01 in. or less in width, these cracks will not be detrimental to the performance of the beam either at service load or at the factored load stage. It should be noted that end-zone stresses in pretensioned and bonded post-tensioned beams do not increase in proportion to loads. The failure stress f_{ps} in the tendon at beam failure is attained only at the maximum moment section.

For *pretensioned members*, based on tests reported in Ref. 19.22, a very simple equation has been proposed for the design of end-zone reinforcement:

$$A_t = 0.021 \frac{P_i h}{f_s l_t} \tag{19.55}$$

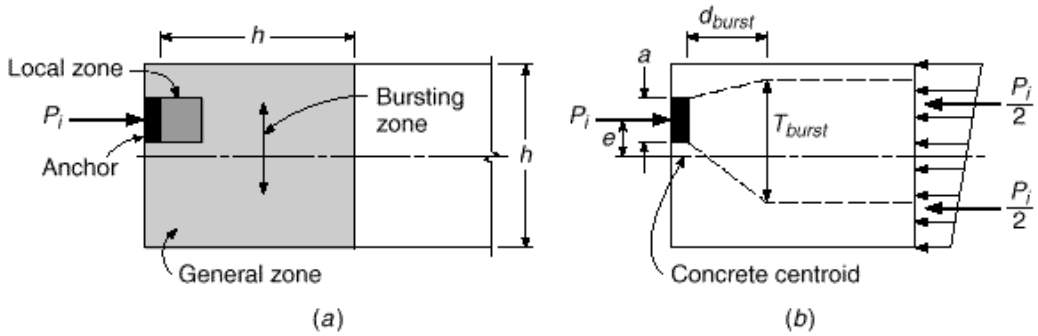

FIGURE 19.27
Post-tensioned end block: (*a*) local and general zone; (*b*) strut-and-tie model.

where A_t = total cross-sectional area of stirrups necessary, in^2
P_i = initial prestress force, lb
h = total member depth, in.
f_s = allowable stress in stirrups, psi
l_t = transfer length, in.

An allowable stress f_s = 20,000 psi has been found in tests to produce acceptably small crack widths. The required reinforcement having total area A_t should be distributed over a length equal to $h/5$ measured from the end face of the beam, and for most efficient crack control the first stirrup should be placed as close to the end face as practical. It is recommended in Ref. 19.22 that vertical reinforcement according to Eq. (19.55) be provided for *all* pretensioned members, unless tests or experience indicates that cracking does not occur at service or overload stages.

For post-tensioned members, the end region is divided into two zones: local and general, as shown in Fig. 19.27*a*. The *local zone* is a rectangular prism immediately surrounding the anchorage device and any confining reinforcement around the device. The *general zone* consists of a region that is approximately one structural depth h from the end of the beam and includes the local zone. For internal anchors, such as used in slabs, the general zone extends a distance h ahead of and behind the anchorage hardware. Stresses in the local zone are determined based on tests. The post-tensioning supplier specifies the reinforcement details for the local zone.

Stress variations in the general zone are nonlinear and are characterized by a transition from the local zone to an assumed uniform stress gradient a distance h from the anchor. Reinforcement in the general zone may be designed by one of three methods. These methods include equilibrium-based plasticity models, such as the strut-and-tie model, linear stress analysis such as finite element analysis, and simplified elasticity solutions similar to the photoelastic model shown graphically in Fig. 19.25 or elasticity analyses described in Ref. 19.23. Simplified equations are not permitted for nonrectangular cross sections, where multiple anchorages are used (unless closely spaced), or where discontinuities disrupt the force flow path.

Strut-and-tie design approaches for highway girder anchorages are detailed in the AASHTO *Standard Specifications for Highway Bridges* (Refs. 19.17 and 19.23). An abbreviated version of the AASHTO Specifications is incorporated in ACI Commentary R18.13. ACI Code 18.15 requires that complex, multiple anchorage systems conform to the full AASHTO Specifications.

For the common case of a rectangular end block and simple anchorage (Fig. 19.27*b*), ACI Commentary 18.13 offers simplified equations based on test results and

strut-and-tie modeling. The magnitude of the bursting force T_{burst} and the location of its centroid distance from the front of the anchor d_{burst} may be calculated as

$$T_{burst} = 0.25\Sigma P_{su}\left(1 - \frac{a}{h}\right) \tag{19.56}$$

and

$$d_{burst} = 0.5h - 2e \tag{19.57}$$

where ΣP_{su} = sum of total factored post-tensioning force
a = depth of anchorage device
e = absolute value of eccentricity of anchorage device to centroid of concrete section
h = depth of cross section

The use of the factored post-tensioning force P_{su} recognizes that the tendon force is acting as a load. Hence, the maximum jacking stress $0.80f_{pu}$ is multiplied by a load factor of 1.2 to calculate P_{su}.

$$P_{su} = 1.2 \cdot 0.80 f_{pu} A_{ps} = 0.96 f_{pu} A_{ps} \tag{19.58}$$

Transverse reinforcement $A_s = T_{burst}/f_y$ is added in a region that is centered on the location d_{burst} to carry the bursting force.

In cases where the simplified equations do not apply, a strut-and-tie model (Chapter 10) or finite element analysis may be required to design the bursting zone.

EXAMPLE 19.7

Design of end-zone reinforcement for post-tensioned beam. End-zone reinforcement is to be designed for the rectangular post-tensioned beam shown in Fig. 19.28. The initial prestress force P_i of 250 kips is applied by two closely spaced tendons having a combined eccentricity of 8.0 in. Material properties are $f'_{ci} = 4250$ psi and $f_y = 60{,}000$ psi.

SOLUTION. The rectangular section and the closely spaced anchorage devices allow the use of the simplified ACI equations.

$$d_{burst} = 0.5h - 2e = 0.5 \cdot 30 - 2 \times 8 = 7 \text{ in.}$$

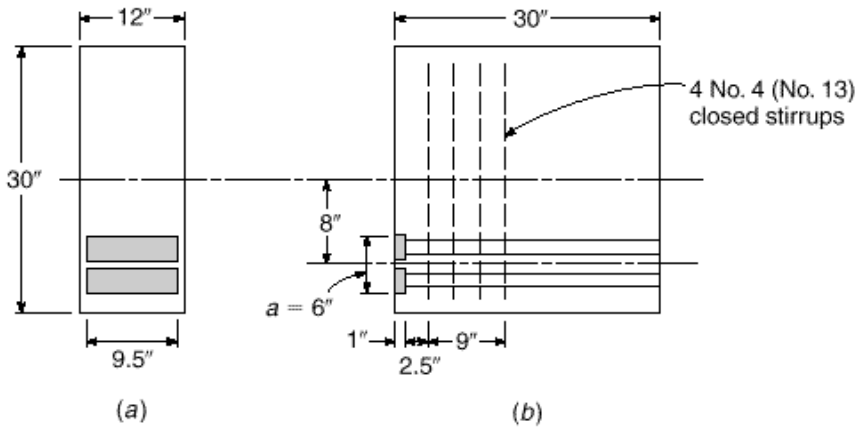

FIGURE 19.28
Design of post-tensioned anchor zone: (*a*) section at end anchors; (*b*) end zone reinforcement.

The initial prestressing force is 250 kips, which corresponds to a tendon stress level of $0.82f_{py}$. The maximum jacking stress level in the tendons is $0.94f_{py}$, or $0.80\,f_{pu}$. In this example, only the initial prestress is provided. Hence, the factored tendon force is calculated as

$$P_{su} = 1.2 \cdot \frac{0.94}{0.82} \cdot 250 = 344 \text{ kips}$$

for which

$$T_{burst} = 0.25\Sigma P_{su} \cdot 1 - \frac{a}{h} \cdot = 0.25 \times 344 \cdot 1 - \frac{6}{30} \cdot = 68.8 \text{ kips}$$

The area of steel needed to resist T_{burst} is

$$A_s = \frac{T_{burst}}{\cdot f_y} = \frac{68.8}{0.85 \times 60} = 1.35 \text{ in}^2$$

Using No. 4 (No. 13) closed stirrups with an area of 2×0.20 in^2 gives

$$n = \frac{1.35}{2 \times 0.20} = 3.4 \text{ stirrups}$$

Four No. 4 (No. 13) closed stirrups will be used. The first stirrup will be placed $2\frac{1}{2}$ in. from the anchor plate, and the other three stirrups will be placed 3 in. on center, as shown in Fig. 19.28*b*, centering the stirrups a distance d_{burst} from the anchor plate. The closed stirrups ensure that anchorage requirements are satisfied. Details of the reinforcement in the local zone are not shown.

19.17 DEFLECTION

Deflection of the slender, relatively flexible beams that are made possible by prestressing must be predicted with care. Many members, satisfactory in all other respects, have proved to be unserviceable because of excessive deformation. In some cases, the absolute amount of deflection is excessive. Often, it is the differential deformation between adjacent members (e.g., precast roof-deck units) that causes problems. More often than not, any difficulties that occur are associated with upward deflection due to the sustained prestress load. Such difficulties are easily avoided by proper consideration in design.

When the prestress force is first applied, a beam will normally camber upward. With the passage of time, concrete shrinkage and creep will cause a gradual reduction of prestress force. In spite of this, the upward deflection usually will increase, due to the differential creep, affecting the highly stressed bottom fibers more than the top. With the application of superimposed dead and live loads, this upward deflection will be partially or completely overcome, and zero or downward deflection obtained. Clearly, in computing deformation, careful attention must be paid to both the age of the concrete at the time of load application and the duration of the loading.

The prediction of deflection can be approached at any of several levels of accuracy, depending upon the nature and importance of the work. In some cases, it is sufficient to place limitations on the span-depth ratio, based on past experience. Generally, deflections must be calculated. (Calculation is required for *all* prestressed members, according to ACI Code 9.5.4.) The approximate method described here will be found sufficiently accurate for most purposes. In special circumstances, where it is important to obtain the best possible information on deflection at all important load

stages, such as for long-span bridges, the only satisfactory approach is to use a summation procedure based on incremental deflection at discrete time steps, as described in Refs. 19.1, 19.8, 19.24, and 19.25. In this way, the time-dependent changes in prestress force, material properties, and loading can be accounted for to the desired degree of accuracy.

Normally, the deflections of primary interest are those at the initial stage, when the beam is acted upon by the initial prestress force P_i and its own weight, and one or more combinations of load in service, when the prestress force is reduced by losses to the effective value P_e. Deflections are modified by creep under the sustained prestress force and due to all other sustained loads.

The short-term deflection Δ_{pi} due to the initial prestress force P_i can be found based on the variation of prestress moment along the span, making use of moment-area principles and superposition. For statically determinate beams, the ordinates of the moment diagram resulting from the eccentric prestress force are directly proportional to the eccentricity of the steel centroid line with respect to the concrete centroid. For indeterminate beams, eccentricity should be measured to the thrust line rather than to the steel centroid (see Ref. 19.1). In either case, the effect of prestress can also be regarded in terms of equivalent loads and deflections found using familiar deflection equations.

The downward deflection Δ_o due to girder self-weight, which is usually uniformly distributed, is easily found by conventional means. Thus, the net deflection obtained immediately upon prestressing is

$$\cdot = - \cdot_{pi} + \cdot_{o} \tag{19.59}$$

where the negative sign indicates upward displacement.

Long-term deflections due to prestress occur as that force is gradually reducing from P_i to P_e. This can be accounted for in an approximate way by assuming that creep occurs under a constant prestress force equal to the average of the initial and final values. Corresponding to this assumption, the total deflection resulting from prestress alone is

$$\cdot = - \cdot_{pe} - \frac{\cdot_{pi} + \cdot_{pe}}{2} C_c \tag{19.60}$$

where

$$\cdot_{pe} = \cdot_{pi} \frac{P_e}{P_i}$$

and C_c is set equal to the ultimate creep coefficient C_u for the concrete (see Table 2.1).

The long-term deflection due to self-weight is also increased by creep and can be obtained by applying the creep coefficient directly to the instantaneous value. Thus, the total member deflection, after losses and creep deflections, when effective prestress and self-weight act, is

$$\cdot = - \cdot_{pe} - \frac{\cdot_{pi} + \cdot_{pe}}{2} C_c + \cdot_{o} \cdot 1 + C_c \cdot \tag{19.61}$$

The deflection due to superimposed loads can now be added, with the creep coefficient introduced to account for the long-term effect of the sustained loads, to obtain the net deflection at full service loading:

$$\cdot = - \cdot_{pe} - \frac{\cdot_{pi} + \cdot_{pe}}{2} C_c + \cdot\cdot_{o} + \cdot_{d} \cdot 1 + C_c \cdot + \cdot_{l} \tag{19.62}$$

TABLE 19.5
Deflection and crack width requirements for prestressed concrete members

	Class		
Condition	U	T	C
Assumed behavior	Uncracked	Transition between cracked and uncracked	Cracked
Deflection calculation basis	Gross section	Cracked section—bilinear behavior	Cracked section—bilinear behavior

where Δ_d and Δ_l are the immediate deflections due to superimposed dead and live loads, respectively.

The selection of section properties for the calculation of deflections is dependent upon the cracking in the section. Table 19.5 defines the appropriate section properties and deflection calculation methodology for Class U, T, and C members (Refs. 19.1, 19.23, and 19.24). Bilinear behavior in Table 19.5 implies that deflections based on loads up to the cracking moment are based on the gross section, and deflections on loads greater than the cracking load are based on the effective cracked section properties (Ref. 19.8).

EXAMPLE 19.8

The 40 ft simply supported T beam shown in Fig. 19.29 is prestressed with a force of 314 kips, using a parabolic tendon with an eccentricity of 3 in. above the concrete centroid at the supports and 7.9 in. below the centroid at midspan. After time-dependent losses have occurred, this prestress is reduced to 267 kips. In addition to its own weight of 330 lb/ft, the girder must carry a short-term superimposed live load of 900 lb/ft. Estimate the deflection at all critical stages of loading. The creep coefficient $C_c = 2.0$, $E_c = 4 \times 10^6$ psi, and modulus of rupture = 530 psi.

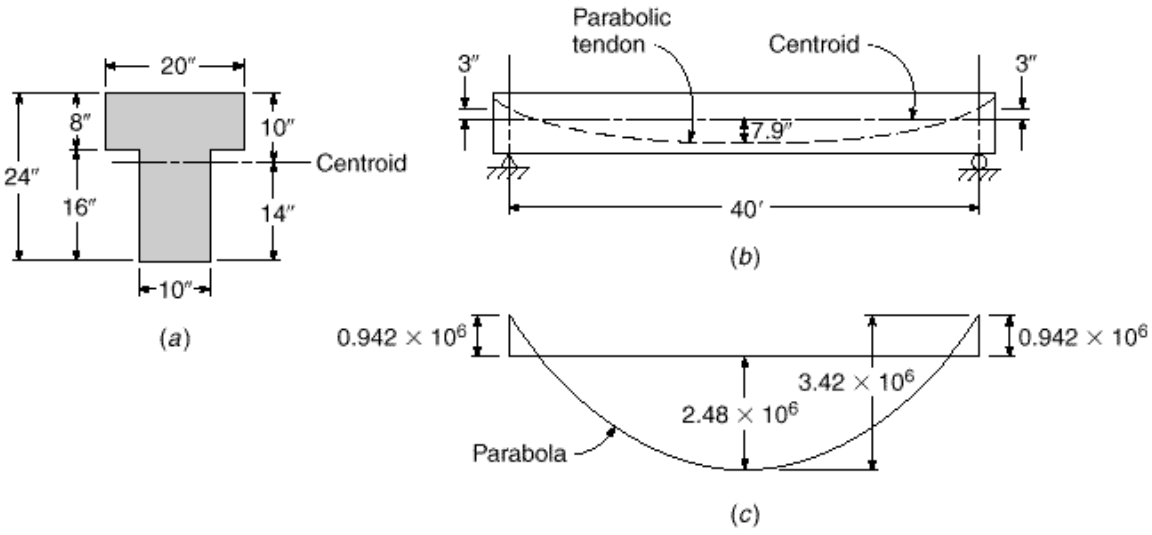

FIGURE 19.29
T beam of Example 19.8: (*a*) cross section; (*b*) tendon profile; (*c*) moment from initial prestressing force (in-lb).

SOLUTION. It is easily confirmed that the stress in the bottom fiber when the beam carries the maximum load to be considered is 80 psi compression, meeting the requirements for a Class U member. All deflection calculations can, therefore, be based on the moment of inertia of the gross concrete section, $I_c = 15{,}800$ in^4. It is convenient to calculate the deflection due to prestress and that due to girder load separately, superimposing the results later. For the eccentricities of the tendon profile shown in Fig. 19.29*b*, the application of $P_i = 314$ kips causes the moments shown in Fig. 19.29*c*. Applying the second moment-area theorem by taking moments of the $M \cdot EI$ diagram between midspan and the support, about the support, produces the vertical displacement between those two points as follows:

$$\Delta_{pi} = \frac{-\tfrac{1}{2} \times 3.42 \times 10^6 \times 240 \times \tfrac{2}{3} \times 240 \times \tfrac{5}{8} + \tfrac{1}{2} \times 0.942 \times 10^6 \times 240 \times 120}{4 \times 10^6 \times 15{,}800} = -0.87 \text{ in.}$$

the minus sign indicating upward deflection due to initial prestress alone. The downward deflection due to the self-weight of the girder is calculated by the well-known equation

$$\Delta_o = \frac{5wl^4}{384EI} = \frac{5 \times 330 \times 40^4 \times 12^4}{384 \times 12 \times 4 \times 10^6 \times 15{,}800} = +0.30 \text{ in.}$$

When these two results are superimposed, the net upward deflection when initial prestress and girder load act together is

$$-\Delta_{pi} + \Delta_o = -0.87 + 0.30 = -0.57 \text{ in.}$$

Shrinkage and creep of the concrete cause a gradual reduction of prestress force from $P_i = 314$ kips to $P_e = 267$ kips and reduce the bending moment due to prestress proportionately. Concrete creep, however, acts to increase both the upward deflection component due to the prestress force and the downward deflection component due to the girder load. The net deflection after these changes take place is found using Eq. (19.60), with $\Delta_{pe} = -0.87 \times 267/314 = -0.74$ in.:

$$\Delta = -0.74 - \frac{0.87 + 0.74}{2} \times 2.0 + \frac{1}{2} \times 0.30 \times 1 + 2.0$$
$$= -0.74 - 1.61 + 0.90 = -1.45 \text{ in.}$$

In spite of prestress loss, the upward deflection is considerably larger than before. Finally, as the 900 lb/ft short-term superimposed load is applied, the net deflection is

$$\Delta = -1.45 + 0.30 \times \frac{900}{330} = -0.63 \text{ in.}$$

Thus, a net upward deflection of about 1/750 times the span is obtained when the member carries its full superimposed load.

19.18 CRACK CONTROL FOR CLASS C FLEXURAL MEMBERS

The service level stress limitations for Class U and T flexural members are sufficient to control cracking at service loads. Class C flexural members must satisfy the crack control provisions for ordinary reinforced concrete members, modified by ACI Code 18.4.4. These requirements take the form of limitations on tendon spacing and on the change in stress in the prestressing tendon under service load.

For Class C prestressed flexural members not subjected to fatigue or aggressive exposure, the spacing of bonded reinforcement nearest the extreme tension face may

not exceed that given for nonprestressed concrete in Section 6.3. Aggressive conditions occur where the tendons may be exposed to chemical attack and include seawater and corrosive industrial environments. In these situations, the designer should increase the concrete cover or reduce the tensile stresses, based on professional judgment, commensurate with the exposure risk.

The spacing requirements for reinforcement in Class C members may be satisfied by using nonprestressed bonded tendons. The spacing between bonded tendons, however, may not exceed two-thirds of the maximum spacing for nonprestressed reinforcement given in Eq. (6.3). When both conventional reinforcement and bonded tendons are used to meet the spacing requirements, the spacing between a tendon and a bar may not exceed five-sixths of that permitted in Eq. (6.3). When applying Eq. (6.3), Δf_{ps} is substituted for f_s, where Δf_{ps} is the difference between the tendon stress at service loads based on a cracked section and the decompression stress f_{dc}, which is equal to the stress in the tendon when concrete stress at the level of the tendon is zero. ACI Code 18.4.4 permits f_{dc} to be taken as the effective prestress f_{pe}. The magnitude of Δf_{ps} is limited to a maximum of 36 ksi. When Δf_{ps} is less than 20 ksi, the reduced spacing requirements need not be applied. If the effective depth of the member exceeds 36 in., additional skin reinforcement along the sides of the member web, as described in Section 6.3, is required to prevent excessive surface crack widths above the main flexural reinforcement.

REFERENCES

19.1. A. H. Nilson, *Design of Prestressed Concrete*, 2nd ed., John Wiley, New York, 1987.
19.2. A. E. Naaman, *Prestressed Concrete Analysis and Design*, McGraw-Hill, New York, 1982.
19.3. T. Y. Lin and N. H. Burns, *Design of Prestressed Concrete Structures*, 3rd ed., John Wiley, New York, 1981.
19.4. J. R. Libby, *Modern Prestressed Concrete*, 3rd ed., Van Nostrand Reinhold, New York, 1984.
19.5. E. G. Nawy, *Prestressed Concrete*, Prentice Hall, Englewood Cliffs, NJ, 2002.
19.6. M. P. Collins and D. Mitchell, *Prestressed Concrete Structures*, Prentice Hall, Englewood Cliffs, NJ, 1991.
19.7. *Post-Tensioning Manual*, 5th ed., Post-Tensioning Institute, Phoenix, AZ, 1990.
19.8. *PCI Design Handbook*, 5th ed., Precast/Prestressed Concrete Institute, Chicago, IL, 1999.
19.9. *Manual for Quality Control for Plants and Production of Precast and Prestressed Concrete*, 4th ed., MNL-116-98, Precast/Prestressed Concrete Institute, Chicago, IL, 1998.
19.10. P. W. Abeles, "Design of Partially Prestressed Concrete Beams," *J. ACI*, vol. 64, no. 10, 1967, pp. 669–677.
19.11. A. H. Nilson, "Discussion of 'Design of Partially Prestressed Concrete Beams' by P. W. Abeles" (Ref. 19.10), *J. ACI*, vol. 65, no. 4, 1968, pp. 345–347.
19.12. P. W. Abeles and B. K. Bardhan-Roy, *Prestressed Concrete Designer's Handbook*, 3rd ed., Cement and Concrete Association, London, 1981.
19.13. ACI Committee 423, *State-of-the-Art Report on Partially Prestressed Concrete* (ACI 423.5R-99), American Concrete Institute, Farmington Hills, MI, 1999.
19.14. CEB-FIP Joint Committee, "International Recommendations for the Design and Construction of Prestressed Concrete Structures," Cement and Concrete Association, London, 1970.
19.15. *Code of Practice for the Structural Use of Concrete*, CP110, British Standards Institution, London, 1972.
19.16. Y. Guyon, *Limit State Design of Prestressed Concrete*, vols. 1 and 2, John Wiley, New York, 1972.
19.17. *Standard Specifications for Highway Bridges*, 17th ed., American Association of State Highway and Transportation Officials, Washington, DC, 2001.
19.18. PCI Committee on Prestress Losses, "Recommendations for Estimating Prestress Losses," *J. Prestressed Concr. Inst.*, vol. 20, no. 4, 1975, pp. 43–75.
19.19. P. Zia, H. K. Preston, N. L. Scott, and E. B. Workman, "Estimating Prestress Losses," *Concr. Intl.*, vol. 1, no. 6, 1979, pp. 32–38.
19.20. J. G. MacGregor and J. M. Hanson, "Proposed Changes in Shear Provisions for Reinforced and Prestressed Concrete Beams," *J. ACI*, vol. 66, no. 4, 1969, pp. 276–288.

19.21. N. W. Hanson and P. W. Kaar, "Flexural Bond Tests of Pretensioned Prestressed Beams," *J. ACI*, vol. 30, no. 7, 1959, pp. 783–802.

19.22. W. T. Marshall and A. H. Mattock, "Control of Horizontal Cracking in the Ends of Pretensioned Prestressed Concrete Girders," *J. Prestressed Concr. Inst.*, vol. 5, no. 5, 1962, pp. 56–74.

19.23. J. E. Breen, O. Burdet, C. Roberts, D. Sanders, G. Wollman, and B. Falconer, "Anchorage Zone Reinforcement for Post-Tension Concrete Girders," NCHRP *Report* 356, Transportation Research Board, National Academy Press, Washington, DC, 1994.

19.24. ACI Committee 435, "Deflection of Prestressed Concrete Members," *J. ACI*, vol. 60, no. 12, 1963, pp. 1697–1728.

19.25. D. E. Branson, *Deformation of Concrete Structures*, McGraw-Hill, New York, 1977.

PROBLEMS

19.1. A rectangular concrete beam with width $b = 11$ in. and total depth $h = 28$ in. is post-tensioned using a single parabolic tendon with an eccentricity of 7.8 in. at midspan and 0 in. at the simple supports. The initial prestress force $P_i = 334$ kips, and the effectiveness ratio $R = 0.84$. The member is to carry superimposed dead and live loads of 300 and 1000 lb/ft respectively, uniformly distributed over the 40 ft span. Specified concrete strength $f'_c = 5000$ psi, and at the time of transfer $f'_{ci} = 4000$ psi. Determine the flexural stress distributions in the concrete at midspan (*a*) for initial conditions before application of superimposed load and (*b*) at full service load. Compare with the ACI limit stresses for Class U members.

19.2. A pretensioned prestressed beam has a rectangular cross section of 6 in. width and 20 in. total depth. It is built using normal-density concrete with a specified strength $f'_c = 4000$ psi and a strength at transfer of $f'_{ci} = 3000$ psi. Stress limits are as follows: $f_{ti} = 165$ psi, $f_{ci} = -1800$ psi, $f_{ts} = 475$ psi, and $f_{cs} = -1800$ psi. The effectiveness ratio R may be assumed equal to 0.80. For these conditions, find the initial prestress force P_i and eccentricity e to maximize the superimposed load moment $M_d + M_l$ that can be carried without exceeding the stress limits. What uniformly distributed load can be carried on a 30 ft simple span? What tendon profile would you recommend?

19.3. A pretensioned beam is to carry a superimposed dead load of 600 lb/ft and service live load of 1200 lb/ft on a 55 ft simple span. A symmetrical I section with $b = 0.5h$ will be used. Flange thickness $h_f = 0.2h$ and web width $b_w = 0.4b$. The member will be prestressed using Grade 270 strands. Time-dependent losses are estimated at 20 percent of P_i. Normal-density concrete will be used, with $f'_c = 5000$ psi and $f'_{ci} = 3000$ psi.

(*a*) Using straight strands, find the required concrete dimensions, prestress force, and eccentricity. Select an appropriate number and size of tendons, and show by sketch their placement in the section.

(*b*) Revise the design of part (*a*) using tendons harped at the third points of the span, with eccentricity reduced to zero at the supports.

(*c*) Comment on your results. In both cases, ACI stress limits are to be applied. You may assume that deflections are not critical and that the beam is Class T at full service load.

19.4. The hollow core section shown in Fig. P19.4 is prestressed with four $\frac{1}{2}$ in. diameter, 270 ksi low-relaxation strands and is simply supported on masonry walls with a span length of 20 ft, center-to-center of the supports. In addition to its self-weight, the section carries a superimposed live load of 225 psf. Material properties are $f'_c = 5000$ psi and $f'_{ci} = 3500$ psi. Determine (*a*) if service load stresses in the section are suitable for a Class U flexural member using $R = 0.82$ and (*b*) if the section has sufficient capacity for the specified loads.

FIGURE P19.4

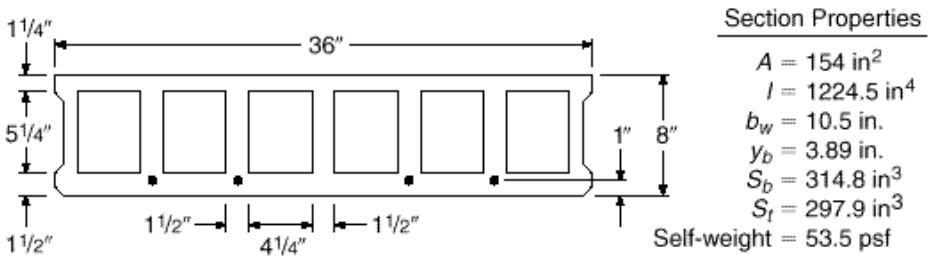

19.5. For the beam in Problem 19.4, make a detailed computation of the losses in the prestressing force. Compare your results to the assumed value of $R = 0.82$.

19.6. Establish the required spacing of No. 3 (No. 10) stirrups at a beam cross section subject to factored load shear V_u of 35.55 kips and moment M_u of 474 ft-kips. Web width $b_w = 5$ in., effective depth $d = 24$ in., and total depth $h = 30$ in. The concrete shear contribution may be based on the approximate relationship of Eq. (19.46). Use $f_y = 60{,}000$ psi for stirrup steel, and take $f'_c = 5000$ psi.

19.7. A symmetrical prestressed I beam having total depth 48 in., flange width 24 in., flange thickness 9.6 in., and web thickness 9.6 in. is to span 70 ft. It is post-tensioned using 18 Grade 270 $\frac{1}{2}$ in. diameter low-relaxation strands in a single tendon having a parabolic profile, with $e = 18$ in. at midspan and zero at the supports. (The curve can be approximated by a circular arc for loss calculations.) The jacking force $P_j = 618$ kips. Calculate losses due to slip, elastic shortening, friction, creep, shrinkage, and relaxation. Express your results in tabular form both numerically and as percentages of initial prestress P_i. Creep effects may be assumed to occur under the combination of prestress force plus self-weight. The beam is prestressed when the concrete is aged 7 days. Anchorage slip = 0.25 in., coefficient of strand friction = 0.20, coefficient of wobble friction = 0.0010, creep coefficient = 2.35. Member properties are as follows: $A_c = 737$ in^2, $I_c = 192{,}000$ in^4, $c_1 = c_2 = 24$ in., $f'_c = 5000$ psi, $E_c = 4{,}000{,}000$ psi, $E_s = 27{,}000{,}000$ psi, $w_c = 150$ pcf, and $C_c = 2.65$.

19.8. The concrete T beam shown in Fig. P19.8 is post-tensioned at an initial force $P_i = 229$ kips, which reduces after 1 year to an effective value $P_e = 183$ kips. In addition to its own weight, the beam will carry a superimposed short-term live load of 21.5 kips at midspan. Using the approximate method described in Section 19.17, find (*a*) the initial deflection of the unloaded girder and (*b*) the deflection at the age of 1 year of the loaded girder. The following data are given: $A_c = 450$ in^2, $c_1 = 8$ in., $I_c = 24{,}600$ in^4, $E_c = 3{,}500{,}000$ psi, $C_c = 2.5$.

FIGURE P19.8